Hyperton-aktivierte Kationen Kanäle in HepG2-Zellen: Rolle in Proliferation und mögliche molekulare Bestandteile

Dissertation zur Erlangung des Grades
eines Doktors der Naturwissenschaften
der Fakultät für Biologie und Biotechnologie
an der Internationalen Graduiertenschule Biowissenschaften
der Ruhr-Universität Bochum

angefertigt im
Max-Planck-Institut für Molekulare Physiologie
Abteilung Epithelphysiologie/Systemische Zellbiologie

Arbeitsgruppe Biophysik und Zellbiologie
Prof. Dr. Frank Wehner

vorgelegt von
Maryna Bondarava

aus
Minsk, Weissrussland

Bochum
November, 2007

Hypertonicity-Induced Cation Channels in HepG2 cells: Role in Proliferation and Putative Molecular Correlates

Dissertation to obtain the degree
Doctor Rerum Naturalium (Dr. rer. nat.)
at the Faculty of Biology and Biotechnology
Ruhr-University Bochum

International Graduate School Biosciences
Ruhr-University Bochum

performed at
Max Planck Institute of Molecular Physiology,
Department of Epithelial Cell Physiology/Systemic Cell Biology

Research Group of Biophysics and Cell Biology
Prof. Dr. Frank Wehner

submitted by
Maryna Bondarava

from
Minsk, Belarus

Bochum
November, 2007

accepted on the recommendation of
Prof. Dr. Frank Wehner, first supervisor
Prof. Dr. Dr. Dr. med. habil. Hanns Hatt, second supervisor

Table of contents

1. INTRODUCTION

1.1 Cell Volume Regulation

Alterations of cell volume participate in the regulation of epithelial transport, metabolism, migration, cell proliferation as well as cell death and they contribute to the pathophysiology of many diseases. Cell volume constancy is challenged by any alterations of intracellular and/or extracellular osmolarity (Lang F. et al., 1998).

With very few exceptions mammalian cell membranes are highly permeable to water, which follows any osmotic pressure gradient. Water permeation occurs by diffusion or through membrane proteins named water channels (Lang F. et al., 1998).

To avoid or counteract alterations of their volume, cells have developed a number of cell volume regulatory mechanisms. When swollen beyond their set point, cells decrease their volume by the release of ions, thus establishing "regulatory volume decrease (RVD)". When shrunken beyond their set point, cells increase their volume by the uptake of ions, thus achieving "regulatory volume increase (RVI)". Ion transport may alter cell membrane potential and thus disturb cellular function. Therefore, cells utilize additionally organic osmolytes for cell volume regulation. Organic osmolyte content is regulated by transport across the

cell membrane and enzymes generating or disposing osmotically active substances (Lang F. et al., 1998).

1.2 Osmoregulation in Liver Cell Function

Liver cell hydration is dynamic and changes within minutes under the influence of anisoosmolarity, hormones, nutrients and oxidative stress. Most importantly, such fluctuations of cell hydration, i.e. of cell volume, act as an independent and potent signal for the regulation of hepatocellular metabolism and gene expression (Häussinger D. and Lang F., 1998). Cell swelling stimulates protein and glycogen synthesis and simultaneously inhibits proteolysis and glycogenolysis; opposite metabolic patterns are triggered by cell shrinkage. Also, in the perfused rat liver, the rate of transcellular bile acid (taurocholate) transport from the sinusoidal space into the biliary lumen is critically dependent upon the hydration state of the hepatocyte (Häussiger D. and Schliess F., 1995).

1.3 Cell Volume Regulation in Human Hepatocytes

Hepatocytes have to fulfill considerable metabolic demands and, accordingly, their plasmalemma is equipped with potent transporters for a variety of compounds. The high rates of some of these transporters and the metabolic processes themselves mean that hepatocytes have had to develop effective

mechanisms of cell volume regulation by which they can readjust their volumes despite continuous hypotonic and hypertonic stress (Graf J., Häussinger D., 1996).

The regulatory processes that enable shrunken cells under hypertonic conditions to (partially) regain their volumes are summarized as a regulatory volume increase (RVI).
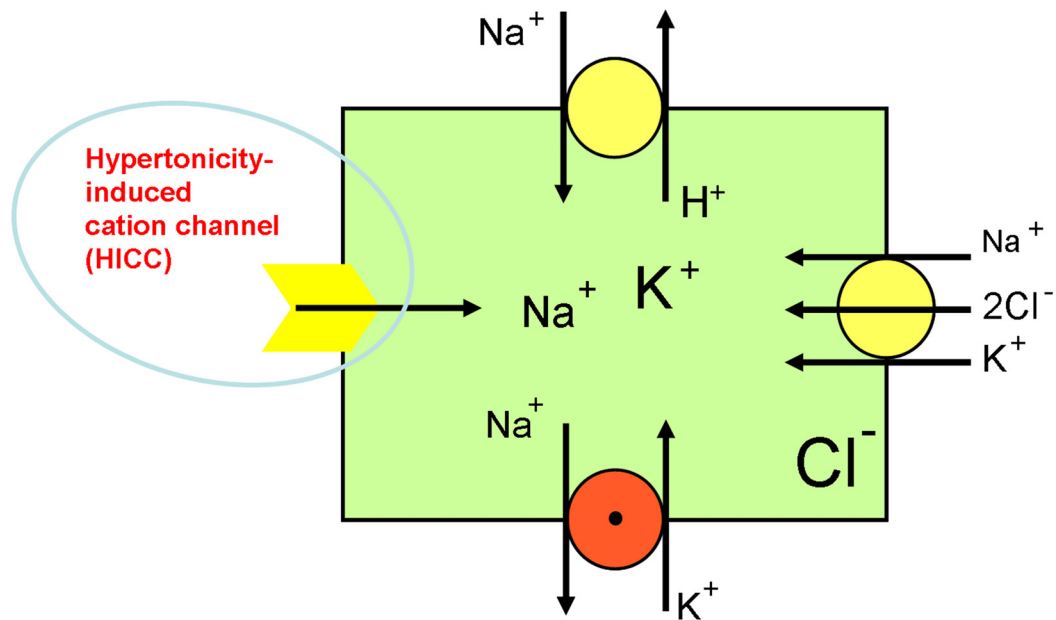
Figure 1.1: Mechanism of RVI in human hepatocytes

In human hepatocytes, hypertonic conditions activate Na^+/H^+ antiport and Na^+-K^+-$2Cl^-$ symport, both mediating an increase of cell Na^+ as the initial event in the RVI process (Figure 1.1). Na^+ is then exchanged for K^+ via stimulation of Na^+/K^+-ATPase so that all three transporters in concert accomplish a net gain of cell K^+. It was shown recently, however, that in primary human hepatocytes hypertonic stress led to a significant increase of cell membrane Na^+ conductance as

well. Moreover, this novel mechanism of conductive Na^+ import could be clearly shown to function as the main mediator of the RVI in this system (Wehner F., Lawonn P., Tinnel H., 2002). Actually, whenever studied in quantitative manner the hypertonic activation of cation channels appears to be the main mechanism of RVI (Wehner F., 2006).

1.3.1 Hypertonicity-Induced Cation Channels in Human Hepatocytes

There is an increasing number of systems from which the hypertonic activation of cation channels is reported. Compared to the symport system, the rates of ion transport by channels are some 4-5 orders of magnitude higher. Accordingly, any modulation of channel activity in response to changes of cell volume will serve as a fast and very efficient regulatory mechanism (Wehner F. et al., 2003).

The novel type of hypertonicity-induced cation channel (HICC) for primary cultures of human hepatocytes was recently described (Li T. et al., 2005) as non-selective for small monovalent cations with permeability ratio for Na^+:Li^+:K^+:Cs^+:$NMDG^+$ of 1:1.2:1.3:1.2:0.6. With a P_{Ca}/P_{Na} of 0.7 the channel is also clearly permeable to Ca^{2+} indicating a possible molecular correlation to transient receptor potential channels (TRPs). Most likely, the channel is Cl^- impermeable but its activity critically depends on the extracellular Cl^- concentration.

The pharmacological characterization of the channel is summarized in Figure 1.2.A. As shown in the figure, with a 64% inhibition by amiloride and a

complete block by flufenamate and Gd^{3+} the HICC appears to represent a molecular link between the amiloride-sensitive and insensitive channels that were reported so far (Li T. et al., 2005).
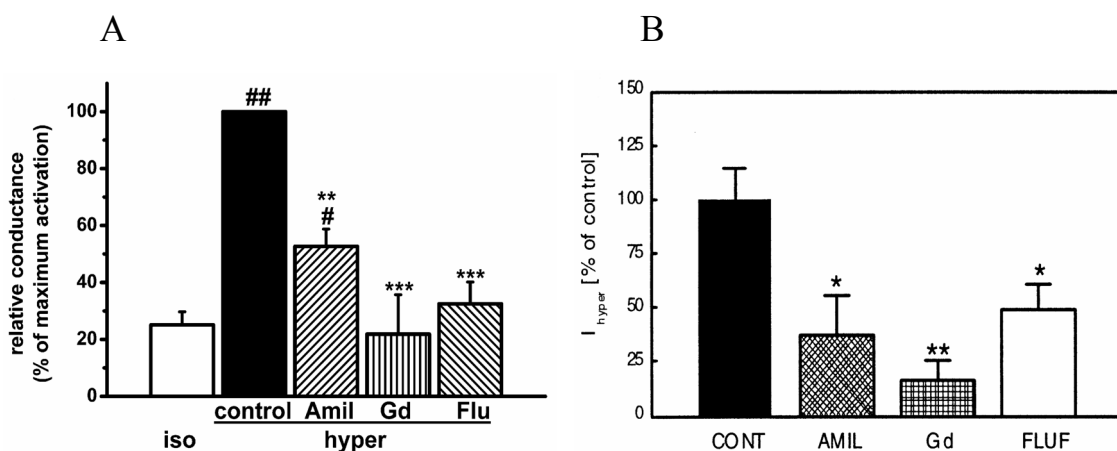
Figure 1.2: Pharmacology of hypertonicity-induced cation channels in primary human hepatocytes (A) and in HepG2 cells (B)

The pharmacological profile of the HICC observed in human hepatoma cell line (HepG2) is very similar to the one in primary hepatocytes (Figure 1.2.B) (Wehner F., Lawonn P., Tinnel H., 2002). Thus, it appears to be very likely that it is the same type of cation channel that is expressed in both systems.

1.3.2 ENaC as a Putative Molecular Correlate of the HICC

Amiloride-sensitivity is one important feature of the epithelial sodium channel (ENaC) which mediates Na^+ uptake across the apical membrane of tight epithelia (Kellenberger S. and Schild L., 2002).

The ENaC is a multimeric protein formed by three homologous subunits: α, β, and γ; each subunit contains only two transmembrane domains. The level of expression of each of the subunits is markedly different in various Na^+ absorbing epithelia raising the possibility that channels with different subunit compositions can actually function in vivo (Carmen M. et al., 1997). A "typical" ENaC is a tetrameric channel with a $\alpha_2\beta\gamma$ stoichiometry, similar to that reported for other cation selective channels, such as K_v, K_{ir}, as well as voltage-gated Na^+ and Ca^{2+} channels that have 4-fold internal symmetry (Kosari F. et al., 1998). α-Subunits can by themselves form functional ENaC channels (Canessa C. M. et al., 1994). Concerning subunit composition, the data from Snyder P. M. indicate that hENaC may contain three α, tree β, and three γ subunits (Snyder P. M. et al., 1998). Kosari F. suggested that α,β-rENaC and α,γ-rENaC are composed of 2 α- and 2 β-subunits or 2 α- and 2 γ-subunits respectively (Kosari F. et al., 1998). The high cation-selectivity and affinity to amiloride as well as the single-channel characteristics of ENaC type of channels are very sensitive to point mutations (Kellenberger S. et al., 1999), changes in subunit composition (Matalon S. et al., 2002) and even to the actual environment conditions of a cell (Askwith C. C. et al., 2001; Jain L. et al., 2001; Ji H. L., et al., 1998; Machida K., et al., 2003).

The degenerin/epithelial Na^+ channel superfamily is a group of structurally related ion channels that are involved in a variety of diverse biological processes beyond Na^+ reabsorption, including chemosensation (Lindemann B., 1996) as well as responses to mechanical stimuli (as postulated for degenerins in *C. elegans*). Indeed, shear stress activates ENaC by modifying the gating properties of the channel (Carattino M. D. et al., 2003). Flow stimulation of ENaC activity and Na^+ absorption is mediated by an increase in hydrostatic pressure and/or membrane stretch (Satlin L. M. et al., 2001). Moreover, amiloride-sensitive stretch activation

has been demonstrated in B lymphocytes (Achard L. M. et al., 1996), bovine α-ENaC or αβγ rENaC in planar lipid bilayers (Awada M. S. et al., 1995), and reconstituted α-ENaC from osteoblasts (Kizer N. et al., 1997).

Conflicting evidence has been reported so far for a possible role of the ENaC in cell volume regulation. Nevertheless, given the restricted tissue distribution of ENaC, is it plausible that ENaC could play an important role in cell volume regulation in response to anisoosmotic stimuli in vivo. This hypothesis is supported by the observation that ENaC mRNA expression in rat medullary ascending limbs was stimulated by acute exposure to hyperosmolality (Machida K. et al., 2003).

Altogether, these observations suggest a possible correlation between the HICC and the ENaC. The HICC maybe formed through α-ENaC together with β- and γ-ENaC or other unknown partners with a stoichiometry different from the classical ENaC.

1.3.3 ENaC and HICC in Rat Hepatocytes

Rat hepatocytes were the first system from which amiloride-sensitive sodium currents in response to hypertonic stress were reported (Wehner F. et al., 1995). Moreover, all three ENaC subunits are expressed in these cells (Böhmer C. et al., 2000). It could then be shown that injection of anti-α anti-sense oligo-DNA into rat hepatocytes reduced hypertonicity-induced currents by 70% (Böhmer C. and Wehner F., 2001).

Specific siRNA constructs directed against α-, β-, and γ-rENaC significantly reduced amiloride-sensitive HICC currents in primary rat hepatocytes. Likewise, the process of RVI was inhibited with the same profile of efficiency, altogether

rendering a functional correlation between the HICC and the three subunits of ENaC very likely (Plettenberg S. et al., 2007).

1.3.4 HICC and TRP Channels

As the hypertonicity-induced cation channel in human hepatocytes represents a combined pharmacology which includes also the sensitivity to the blockers of non-selective cation channels (Gd^{3+}, flufenamate), permeability to the small inorganic cations and Ca^{2+} this may reflect a molecular link between the large group of TRP channels. Transient receptor potential (TRP) channels are unique cellular sensors responding to a wide variety of extra- and intracellular signals, including mechanical and osmotic stress. Members of TRP superfamily of channels share the common features of six transmembrane segments, varying degrees of sequence homology, and permeability to cations (Venkatachalam K. and Montell C., 2007) .

In recent years, TRP channels from multiple subfamilies have been added to the list of mechano- and/or osmosensitive channels, and it is becoming increasingly apparent that Ca^{2+} influx via TRP channels plays a crucial role in the response to mechanical and osmotic perturbations in a wide range of cell types (Pedersen S. F. and Nilius B., 2007).

The non-selective cation channel TRPC6 is activated by mechanically or osmotically induced membrane stretch/deformation (Spassova M. A. et al., 2006) and, actually, quite a number of TRPV channels are mechano- or volume/osmosensitive. A splice variant of TRPV1, TRPV1b, in which a stretch of 60 amino acids is deleted in the intracellular N-terminal region (Lu G. et al., 2005),

for instance, forms a stretch-inhibited cation channel, and these channels are activated by hypertonic cell shrinkage (Ciura S. and Bourque C. W., 2006; Naeini R. S. at al., 2005). TRPV2 has been described as a stretch-activated channel functioning as a mechanosensor in vascular smooth muscle cells and it also appears to be activated by osmotic cell swelling (Beech D. J. et al., 2004; Muraki K. et al., 2003). TRPV4 was the first TRP channel to be described as a volume-activated, Ca^{2+}-permeable cation channel (Liedtke W. et al., 2000; Nilius B. et al., 2001; Strotmann R. et al., 2000). TRPM7 has been proposed to be directly activated by cell stretch and potentiated by hypotonic cell swelling (Numata T. et al., 2007). Finally, the polycystic kidney disease protein 2 (PKD2 or TPRP2) is involved in mechanosensation in the primary cilia of kidney cells and plays a role in osmosensing (Montalbetti N. et al., 2005). Moreover, it was demonstrated that the HICC in HeLa cells was inhibited by SKF-96365, a selective blocker of TRP channels (Wehner F. et al., 2003).

1.4 Cell Volume Regulation: Role in Apoptosis and Proliferation

In addition to their role in mere cell homoeostasis, the mechanisms of RVI and RVD have proven to contribute to a variety of processes in cell physiology including gene expression, the locomotion of cells, the coordination of transport across the apical and basolateral membranes in epithelia, the triggering of metabolic processes in the liver and, most interestingly, the interplay between cell proliferation and apoptosis. Given the paramount importance of HICCs for the RVI

in most preparations studied so far, it is quite obvious that these channels will have a significant impact on the above processes (Wehner F. et al., 2006).

Cell proliferation and apoptotic cell death are fundamental physiological processes adjusting the number of cells in a given tissue to its functional requirements. Cell proliferation is mandatory for the replacement of cells that are lost by necrosis and apoptosis as well as for the generation of additional cells, when the functional demand is increased. Apoptosis serves to eliminate cells, which have become functionally redundant or potentially harmful. When uncontrolled, cell proliferation and apoptosis give rise to a variety of diseases, such as tumors, organ failure, autoimmune disease and neurodegeneration (Lang F. et al., 1998).

So far, a wide variety of mitogenic factors were shown to activate Na^+/H^+ exchanger and many factors stimulate Na^+-K^+-$2Cl^-$ cotransport (Bianchini L., Grinstein S., 1993; Ritter M., Wöll E., 1996). Cell proliferation has indeed been shown to correlate with increase of cell volume in fibroblasts (Lang F. et al., 1992), mesanglial cells (Yamamoto T. et al., 1991), lymphocytes (Dingley A. J. et al., 1994), HL-60 cells (Burger C. et al., 1994), GAP A3 hybridoma cells (Needham D., 1991), smooth muscle cells (Feltes T. F. et al., 1993), and HeLa cells (Takahashi A. et al., 1993).

It is well known that stimulation of cellular osmolyte uptake is an early response to growth factors and that it is important for mitogenesis (Rozengurt E., 1986). For example, a rapid and transient Na^+ and amino acid influx is essential for the mitogenic response of rat hepatocytes (Koch K. S., Leffert H. L., 1979; Freeman T. L. et al., 1999) and 3T3 fibroblasts to growth factors. Also, activation of Na^+-K^+-$2Cl^-$ cotransporter (NKCC1) was shown to be essential for cell cycle progression in 3T3 fibroblasts (Bussolati O. et al., 1996) and human lung cancer

(Iwamoto L. et al., 2004). Moreover, overexpression of NKCC1 in 3T3 fibroblasts induced proliferation and led to a transformed phenotype (Panet R., Atlan H., 2000).

In line with a role of cell swelling in cell cycle progression, hypoosmotic volume increase was sufficient to activate the MAP-kinases Erk-1/Erk-2 and the PI 3-kinase in many cell types, which are known to play a major role in mitogenic cell signaling. Indeed, hypoosmotic treatment of HepG2 cells potentiated proliferation of the cells, which depended on PI 3-kinase-meditated AP1 activation. These results indicate that cell swelling *per se* may be sufficient to promote cell proliferation (Schliess F., Häussinger D., 2005).

Moreover, cell swelling appears to counteract with the process of apoptosis. Hypoosmotic swelling inhibits TGF-β-induced apoptosis in H4IIE rat hepatoma cells, which was independent from NF-κB activation in these cells (Michalke M. et al., 2000). A brief hypoosmotic exposure protected cardiomyocytes from doxorubicin-induced apoptotic volume decrease (AVD) and apoptosis, and this effect was observed even if doxorubicin was applied 60 min after the osmotic pulse (d'Anglemont-de-Tassigny A. et al., 2004).

The early event of cell shrinkage at the beginning of apoptosis (AVD) is a prerequisite for the apoptotic machinery. Accordingly, the Src-like kinase Lck mediates both, the activation of the outwardly rectifying chloride channel (ORCC) and the inhibition of Na^+/H^+ exchange which is the base of the shrinkage of Jurkat cells by CD95 ligand (Lang F. et al., 2000). Interestingly, Lck activity also accounts for the hypoosmotic activation of ORCC that is involved in RVD (Lepple-Wienhues A. et al., 1998).

Hyperosmotic shrinkage does not necessarily trigger apoptosis. For example, efficient RVI could protect cells from hyperosmotic apoptosis. It was shown that

hyperosmotic shrinkage of different lymphoid cells (S49 Neo, CEM-C7, primary thymocytes) is not counteracted by RVI and triggers apoptosis, whereas hyperosmotically treated L-, COS-, HeLa, and GH(3) cells effectively performed RVI and were protected from apoptosis (Bortner C.D., Cidlowski J.A., 1996). Furthermore, inhibition of Na^+/H^+ exchange in a human renal proximal tubule cell line increased the sensitivity towards hyperosmotic apoptosis. This was accompanied by a caspase-dependent degradation of the Na^+/H^+ exchanger NHE1. NHE1 degradation is also obligatory in staurosporine-induced apoptosis in these cells, suggesting that the impairment of mechanisms antagonizing cell shrinkage may be a general feature of apoptosis induction (Wu K.L. et al., 2003).
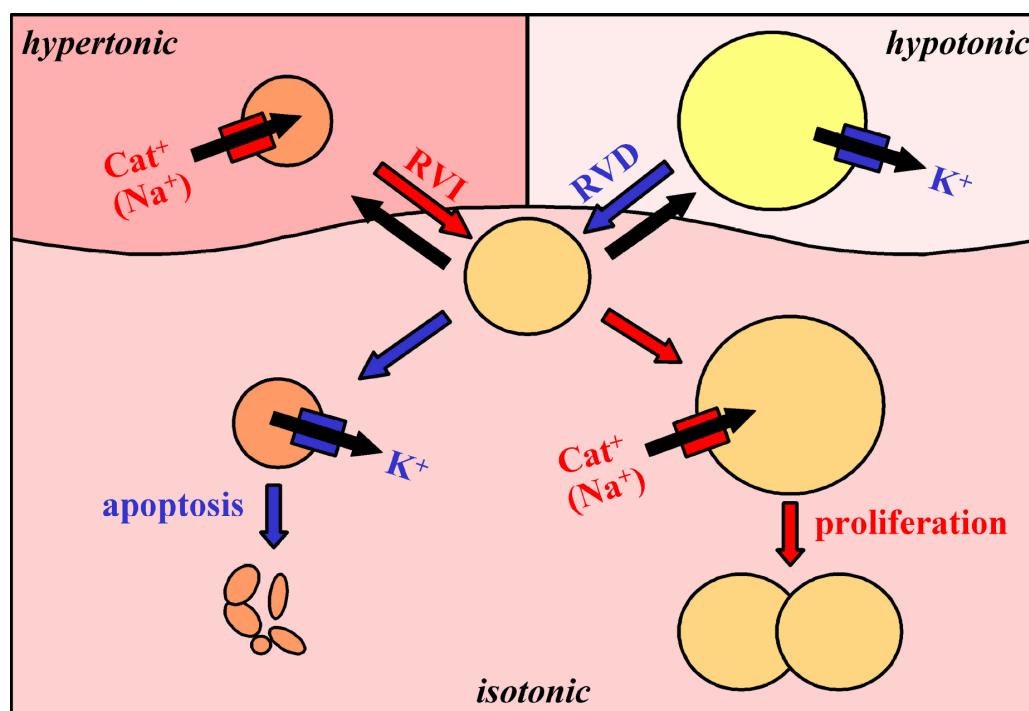
Figure 1.3: Cell volume regulation vs. proliferation and apoptosis (see text for details)

Taken together, convincing evidence has been reported which proves the interplay of the RVI process and its major players with cells proliferation and apoptosis. This hypothesis is summarized in Figure 1.3: isotonic cell shrinkage is one of the very early events in the induction of apoptosis, the programmed cell death; this shrinkage employs the same K^+ channels that mediate the RVD of a cell under hypotonic stress. Accordingly, non-selective cation channels, which are the main mechanism of RVI under hypertonic stress, may by part of the machinery of cell proliferation – as the process opposite to apoptosis. As the hypertonicity-induced cation channel is the main mechanism of RVI in rat and human hepatocytes, no wonder then that it may function as a very efficient mediator of cell proliferation in this system.

1.5 Aims of this Work

In many systems, the activation of hypertonicity-induced cation channels (HICCs) is the most effective mechanism of regulatory volume increase (RVI). Moreover, cell growth and progression through the different phases of the cell cycle were found to require an increase in cell volume. The aims of the present study were to characterize the HICC in HepG2 cells and to test for its contribution to cell proliferation.

Evidence has been reported that the α-subunit of the epithelial sodium channel (ENaC) is a possible molecular correlate of the HICC. Application of small interfering (si)RNA technique was used to test the actual contribution of ENaCs to HICCs and their role in cell proliferation. Furthermore, the actual role of the HICC in the RVI process was supposed to be defined by measurements of cell volume. The novel method of Scanning Acoustic Microscopy was employed for this purpose.

Finally, the overall HICC architecture was supposed to be investigated by implication of biochemical approach.

2. Materials and methods

2.1 Cell Biology Methods

2.1.1 Cell Culture

HepG2 cells (kindly provided by Dr. D. Keppler, DKFZ, Heidelberg) were maintained in RPMI Medium 1640 (Invitrogen, Karlsruhe) with 10% fetal calf serum (FCS) in the presence of penicillin (100 µg/ml) and streptomycin (100 µg/ml) (Invitrogen) under standard culture conditions (5% CO_2, 37 °C). The cells were cultured in 75-cm^2 cell culture flasks (BD Falcon, Heidelberg) until they formed a confluent monolayers and passaged once per week. Detachment of cells from the support was achieved by use of TrypsinEDTA (Invitrogen, Karlsruhe). The passages of cells used for the experiments in this thesis were from 3 to 17.

2.1.2 Transfection of HepG2 Cells

2.1.2.1 Transfection of the siRNA

Gene silencing was performed using sequence specific α-ENaC-siRNA duplexes (sense r(GCACCUUUGGCAUGAUGUA)d(TT) and antisense

r(UACAUCAUGCCAAAGGUGC)d(AG)) conjugated with Alexa Fluor 488. The non-silencing siRNA (sense r(UAUUGGCUUACGCGCAGAU)d(TT) and antisense r(AUCUGCGCGUAAGCCAAUA)d(AG), 3`-Alexa Fluor 488) was used as a negative control. The siRNA duplexes were purchased from QIAGEN (Hilden).

Cells were seeded in 12-well plastic plates 24 hours prior to transfection to achieve 30-50 % confluency. The siRNA duplexes were delivered into the cells by use of DharmaFECT 1 transfection reagent (Perbio Science, Bonn) according to the protocol supplied by the manufacture. The transfection complexes were removed after 6 hours of incubation time and replaced with the culture growth medium. The experiments were performed 26-48 hours after transfection.

2.1.2.2 Transfection of the Vector

2.1.2.2.1 Transient Transfection of HepG2 Cells

For the transient expression of recombinant proteins, HepG2 cells were transfected with plasmid DNA using the Effectene Transfection Kit (QIAGEN, Hilden) following an optimized protocol on the basis of the manufacturer's instructions. 2×10^5 cells were seeded in 12-well plates and grown for 24 hours to reach 60-70% confluency. Cells were then transfected using 10 µl Effectene reagent per each µg of DNA. Transfection complexes were removed and exchanged with growth medium 6 hours thereafter. The experiments were performed 24-28 hours following the transfection procedure.

2.1.2.2.2 Stable Transfection of HepG2 Cells

For the stable expression of the recombinant proteins in HepG2 cells the transfection protocol was the same as for the transient expression (2.1.2.2.1). 24-48 hours after transfection, the cells were seeded in the selective medium (RPMI-1640, 10 % FCS, 1 % ampicillin/streptomycin, 1 mg/ml G-418 (Merck Bioscience, United Kingdom)) and maintained until colonies appeared. For the maintenance of the stably transfected cell line, the concentration of G-418 was reduced down to 0.5 mg/ml.

2.1.3 Crosslinking of Membrane Proteins

The homobifunctional primary amine-reactive crosslinking reagent used in this study was 3,3′-dithiobis (sulfosuccinimidylpropionate) (DTSSP) (Perbio Science, Bonn). It is a water-soluble, thiol-cleavable, membrane impermeable agent that has been used by many investigators so far.

90 % confluent HepG2 cells stably transfected with Flag- or His-tagged α-ENaC were washed twice with PBS to remove media. Freshly dissolved DTSSP in the reaction buffer (PBS) was added to the cells to a final concentration of 1 – 2 mM. Then, the reaction mixture was incubated at room temperature for 30 minutes. Untreated crosslinker was quenched by the addition of 10-20 mM Tris-HCl (pH 7.5) for 15 minutes at room temperature.

2.1.4 Membrane Preparations from HepG2 Cells

HepG2 cells were washed 2 times with ice-cold wash buffer (300 mM NaCl, 50 mM sodium phosphate, 10 mM imidazole, pH 8.0) supplemented with 0.25 M sucrose and protease inhibitor cocktail for use with mammalian cells and tissue extracts (Sigma-Aldrich, Taufkirchen). The cells were scraped with the same buffer from the plates with the aid of a rubber policeman and suspended. The suspension was equilibrated in a high-pressure chamber (Parr Instrument model 4639) with 900 lb./in.^{2} nitrogen at 4°C for 15 min. The cell suspension was rapidly expanded against atmospheric pressure and centrifuged at 850 g for 10 minutes to remove cell debris and nuclei. The supernatant was layered on top of a 4-ml sucrose cushion (40 % sucrose in wash buffer with 0.25 M sucrose) and centrifuged for 45 min at 100,000 g in a swinging bucket rotor. The interphase between the 40 % sucrose and the 0.25 M sucrose layers was collected (membrane fraction) and then centrifuged for 30 min at 45,000 g. The membrane pellet was resuspended in the wash buffer supplemented with 1 % Triton X-100 and protease inhibitor cocktail for mammalian cells (Sigma-Aldrich, Taufkirchen) and incubated at 4°C for 30 min under vigorous shaking. The non-solubilized material was spun down at 45,000 g for 60 min at 4°C. The clear supernatants representing the membrane protein fraction were subjected to the pull-down experiments (2.3.4).

2.2 Molecular biology methods

2.2.1 Preparation of cDNA of α-ENaC Subunit

Total cellular RNA was isolated from HepG2 cells by RNeasy Mini Kit from QIAGEN (Hilden) according to the manufacture's protocol. RNA concentration and quality were assessed spectrophotometrically using a Beckman Coulter DU 800 (USA, CA, Fullerton). RNA (1 µg) was reversely transcribed using 50 U of Superscript II RNase H- Reverse Transcriptase (Invitrogen, Karlsruhe) in a 22 µl reaction volume containing 0.5 µg/µl oligo(dT), 10 mM dNTP mix, 10×RT buffer, 25 mM MgCl2, 0.1 M dithiothreitol, and RNaseOUT Recombinant RNase Inhibitor (Invitrogen, Karlsruhe). The mixture of RNA and oligo(dT) was heated at 65°C for 5 min, chilled on ice, then all other reagents were added and the RT-PCR was conducted at 42°C for 50 min and 70°C for 15 min. The RNase H treatment was performed for 20 min at 37°C.

2.2.2 Polymerase Chain Reaction (PCR)

DNA fragments were amplified *in vitro* by polymerase chain reaction (PCR) after Mullis (Mullis K. et al., 1986). PCR reactions were prepared in a volume of 50 µl. 5 U Taq DNA polymerase (Eppendorf, Hamburg) were mixed with 1x reaction buffer, 0.2 mM of every dNTP, 300 pM of each primer (table 2.1) and 50 ng of DNA template. The PCR reaction was performed in a Mastercyler Gradient thermocycler (Eppendorf, Hamburg) using the following program: 1 cycle 2' at 94

°C, 25-35 cycles with 15'' at 94 °C, 30'' at 50-65 °C (depending on the melting temperature of the primers) and Te at 68 °C (Te = elongation time, dependent on the size of the DNA fragment), 1 cycle 3' at 68 °C. PCR products were analyzed by agarose gel electrophoresis and purified by elution from agarose gels using the QIAquick gel extraction kit (QIAGEN, Hilden) or with the QIAquick spin kit, respectively, according to the manufacturer's protocol.

2.2.3 Quantitative Real-Time PCR (RT-PCR)

Quantitative Real-Time PCR (RT-PCR) was conducted using an Applied Biosystems GeneAmp 5700 Sequence Detection System and a QuantiTech SYBR Green PCR kit (QIAGEN, Hilden) according to the manufacturer's instructions. All PCR reactions were performed in 96-well optical plates (Applied Biosystems, Darmstadt) containing 0.9 µM of each specific forward and reverse primer (table 2.1), 30 – 100 ng of cDNA, and 12.5 µl of SYBR Green I in a total reaction volume of 25 µl. Each run included a buffer blank and no-template control to test for contamination of assay reagents.

2.2.4 Mutagenesis PCR

α-ENaC was tagged with the Flag reporter octapeptide (DYKDDDDK) and with 6 x His tag which replaced the sequence $T^{169}LVAGS^{174}$ corresponding to the extracellular loop of the protein. The introduction of the epitopes was done by use of QuickChange XL Site-Directed Mutagenesis Kit (Stratagene, USA). The 50 µl

reaction mixture contained 1x reaction buffer, 50 ng of dsDNA template, 125 ng of each primer (table 2.1), 1 µl of dNTP mix, 3 µl of QuickSolution and 2.5 U of PfuTurbo DNA polymerase. The PCR reaction was performed in a Mastercyler Gradient thermocycler (Eppendorf, Hamburg) with the following program: 1 cycle 1' at 95 ^{o}C, 18 cycles with 50'' at 95 ^{o}C, 50'' at 60 ^{o}C, 8' (depends on the plasmid length) at 68 ^{o}C, 1 cycle 7' at 68 ^{o}C. Digestion of the amplification products was done by Dpn I restriction enzyme treatment (10 U) for 1 hour at 37 ^{o}C.

2.2.5 Endonuclease Restriction of DNA

For the restriction of DNA plasmids and PCR fragments, endonuclease restriction enzymes from NEB were used in the appropriate buffer. 5-20 units of enzyme per µg of DNA were added to the reaction mixture with a volume of 10-20 µl. If not indicated differently in the manufacturer's protocol, the restriction reaction was performed for 1 hour (or more) at 37 °C and subsequently followed by inhibition of the enzyme for 10 minutes at 65 °C. DNA vectors were afterwards dephosphorylated using 0.5 U/µg DNA calf intestine phosphatase (NEB) at 37 °C for 1 hour to reduce religation of the cleaved vectors.

2.2.6 Ligation

T4-DNA ligase (Invitrogen, Karlsruhe) was used for the ligation of DNA fragments into the vector pcDNA3.1(+). The reaction samples with a final volume of 10-20 µl contained 1x reaction buffer, 1-2 µl T4-DNA ligase and 0.01-0.1 µg of

total DNA. The ligation was performed at 16 °C over night and then analyzed by agarose gel electrophoresis. 1-2 µl of the ligation product was used for the transformation of competent *E. coli* cells (2.2.8).

2.2.7 Transformation

Transformation of One Shot TOP10 Chemically Competent Cells (Invitrogen, Karlsruhe) was carried out following the instructions of the manufacturer. 50 µl of Chemically competent TOP10 (Invitrogen) *E. coli* cells were transformed with a 42 ^{o}C heat shock for 30 sec. After transformation, the cells were diluted with S.O.C. medium (2% Tryptone, 0.5% Yeast Extract, 0.4% glucose, 10 mM NaCl, 2.5 mM KCl, 5 mM $MgCl_2$, 5 mM $MgSO_4$.) to obtain 250 µl. After incubation for 1 hour at 37 °C, the cells were spread at different concentrations on LB plates containing the appropriate antibiotics. Thereafter the plates were incubated at 37 °C for 12-16 hours.

The Endofree Plasmid Maxi Kit and QIAprep Spin Miniprep Kit from QIAGEN (Hilden) were employed for the isolation of purified DNA plasmids from *E.coli* cultures.

2.2.8 Agarose Gel Electrophoresis

DNA restrictions, ligations and PCR products were analyzed by agarose gel electrophoresis using the RAGE RGX-100 system from Cascade Biologics (Portland, USA) according to the manufacturer's instructions. The DNA samples

were diluted in 1xDNA sample buffer (10x: 50 % w/v glycerol, 0.1 % w/v Orange G, 0.1 mM EDTA, pH 7.4) and loaded on 0.8 - 2.0 % agarose gels in 1x TAE buffer (50x: 2 M Tris-acetate, 0.5 M EDTA, pH 8.0) containing 0.5 µg/ml ethidiumbromide. Separation was achieved at 275 V for 15-20 minutes. Agarose gels were subsequently analyzed with a Gel Doc 1000 system (Bio-Rad, Munich). DNA fragments from agarose gel were purified with the QIAEX II Gel Extraction Kit (QIAGEN).

2.2.9 DNA Sequencing

DNA sequencing was performed based on the principle of Sanger (Sanger F. et al., 1977) with the BigDye™ Terminator Kit (Applied Biosystems, USA). Samples of 20 µl containing 300 ng template DNA, 5 pmol sequencing primer and 4µl BigDyeTM Terminator mix were prepared. The sequencing PCR was carried out in a Mastercycler gradient thermocycler (Eppendorf, Hamburg) according to the following program: 1 minute at 94 °C, pursued by 25 cycles with 15 seconds at 94 °C, 30 seconds at T_A and 4 minutes at 60 °C. The annealing temperature T_A is dependent on the melting temperature of the employed primer.

For the removal of unincorporated dye, terminators from sequencing reaction DyeEx 2.0 Spin Kit (QIAGEN, Hilden) were used.

2.3 Biochemical Methods

2.3.1 Protein Determination

The concentration of proteins in cell lysates were determined by two methods: using the standard protocol of Bradford according to Bradford M. M. (1976) and with the Micro BCA^{TM} Protein Assay Kit (Perbio Science, Bonn) according to the protocol supplied by the manufacture. For both techniques, bovine serum was used as the protein standard.

2.3.2 SDS-PAGE

Proteins were separated by discontinuous SDS-PAGE on 8-12 % acrylamide gels with the Nu-PAGE® Bis-Tris Electrophoresis System (Invitrogen, Karlsruhe). Samples were diluted in 5× sample buffer (50 mM Tris, 10% SDS, 0.02% bromphenol blue, 10% glycerol and 2.5 % β-mercaptoethanol). MES SDS running buffer was prepared as 20× stock solution (50 mM MES, 50 mM Tris, 0.1 % SDS and 1 mM EDTA, pH 7.3) and diluted directly before use. As molecular weight marker, the SeeBlue® Plus2 pre-stained standard from Invitrogen (Karlsruhe) has been used. Gels were run at 200 V for 55 min.

2.3.3 Western Blotting

Proteins separated by SDS-PAGE were transferred to PVDF membranes (Bio-Rad Laboratories, Munich) by electrophoresis. After equilibration of the gel, methanol activated PVDF membrane, blotting pads and filters in transfer buffer (20 mM Tris-HCl, 150 mM Glycin, 20% (v/v) Methanol, 0.05% SDS, pH 8.3), the components were placed in the XCell IITM Blot Module according to the manufacturer's instructions (Invitrogen, Karlsruhe). Transfer occurred at a constant current of 180 mA for 45 min. Thereafter, the membrane was blocked in a solution of 5% non-fat dry milk and 1 % BSA in TBST (137 mM NaCl, 2.7 mM KCl, 20 mM Tris-HCl pH 7.4, 0.1% Tween 20) over night at 4°C. Binding of primary and HRP-coupled secondary antibody to the membrane occurred in the blocking solution. Primary antibody dilution varied from 1:100 to 1:1000 (see table 2.2). The secondary antibody was diluted 1:10,000. Following incubation of the membrane with ECL, X-ray films were developed by chemoluminescence.

2.3.4 Pull-down Experiments

The pull-down experiments were performed by use of ANTI-FLAG M2 affinity resin (Sigma-Aldrich, Taufkirchen) in case of the Flag-tagged α-ENaC, or Ni-NTA His-Bind Resin (Merck Chemicals Ltd, United Kingdom), for the His-tagged of α-ENaC, following the protocols supplied by the manufacturers. The bound proteins were eluted with 2x sample buffer (125 mM Tris-HCl, pH 6.8, 4 % SDS, 20 % glycerol, 0.004 % bromphenol blue) and subjected to 1D or 2D electrophoresis.

Alternatively, proteins bound to the resin were digested with 0,01 mg/ml Trypsin in 25 mM NH_4HCO_3 overnight at 37 ^{o}C and further subjected to the electrospray ionisation mass spectrometry (ESI-MS).

2.3.5 2D Electrophoresis

Two-dimensional electrophoresis was used for the analysis of the α-ENaC protein complex eluted from the resin. This technique sorts proteins according to two independent properties in two discrete steps: the first dimension step, isoelectric focusing, separates proteins according to their isoelectric points; the second dimension step, SDS-PAGE, separates proteins according to differences in their molecular mass. In this way information on protein characteristics such as the pI and the apparent molecular mass can be obtained. The first-dimension separation procedure involves IPG strip rehydration, sample application and isoelectric focusing. For IEF the ZOOM IPGRunner[TM] System with rehydrating ZOOM Strips with pH 3-10 and length of 7 cm from Invitrogen (Karlsruhe) was used. The samples were solubilized in the rehydration solution containing 8 M urea, 2 % CHAPS, 20 mM DTT, 0.5 % ZOOM Carrier Ampholytes pH 3-10, 0.002 % bromophenol blue. The solution was applied to the reservoir slots of the ZOOM IPGRunner[TM] Cassette for the IPG strips rehydration (overnight by room temperature). After that the ZOOM IPGRunner[TM] Mini-Cell was assembled and ready for the IEF. The parameters used for isoelectric focusing of protein samples were the following: 200 V for 20 minutes, 450 V for 15 minutes, 750 V for 15 minutes, 2,000 V for 30 minutes.

After IEF the second dimension separation was performed as described in 2.3.2. For SDS-PAGE, the IPG strips were equilibrated in the solution containing 1XNuPAGE LDS Sample Buffer and 1XNuPage Sample Reducing Agent, and then alkylated in the solution containing 1XNuPAGE LDS Sample Buffer with 125mM iodoacetamide.

2.3.6 Staining of Polyacrylamide Gels

2.3.6.1 Coomassie Staining

After electrophoresis, the gels were incubated for 20 minutes in the fixing solution (25 % isopropanol, 10 % acetic acid), then stained for 15 minutes in the staining solution (45 % methanol, 10 % acetic acid, 0.1 % Coomassie Blue R-250). Thereafter, the gels were shortly washed in distilled water and kept 4-5 hours in the destaining solution (20 % ethanol, 5.6 % acetic acid).

2.3.6.2 Silver Staining

2D gels were stained with SilverSNAP Stain for the Mass Spectrometry kit (Perbio Science, Bonn) according to the supplied protocol. After washing in ultrapure water, the gels were incubated two times for 15 minutes in the fixing solution (30 % ethanol, 10 % acetic acid), then two times washed for 5 minutes with ethanol (10 %). Thereafter, the gels were incubated for 1 minute in the

1XSilverSNAP Sensitizer, washed with water and then incubated for 5 minutes in the mixture of SilverSNAP Enhancer and SilverSNAP Stain. After short washing with the water, the gels were placed in the developing solution (SilverSNAP Enhancer with SilverSNAP Developer) until protein spots appeared (2-3 minutes). When the desired band intensity was reached, developer working solution was replaced with stop solution (5 % acetic acid) for 10 minutes.

2.4 Electrophysiological Techniques

2.4.1 Experimental Setup

HepG2 cells were cultured as monolayers in 12-well plastic plates as described in 2.1.1. They were then mechanically detached from the plastic plates by a jet-stream of culture medium, as it was described previously for HeLa cells (Kubo M. and Okada Y., 1992), placed in a glassbottomed chamber of 0.3 ml volume. After they had attached to the glass for to 5 – 10 minutes, the cells were perfused with the respective bathing solutions by gravity at a flow of around 5 ml min^{-1}. Hypertonicity was achieved by addition of 110 mosmol/l of Mannitol. siRNA transfected cells were visualized using an inverted fluorescence microscope (Axiovert 40 CFL, Karl Zeiss, Jena) equipped with a filter set suitable for Alexa Fluor 488 detection (Zeiss filter set 10, excitation BP 450 – 490 nm, emission BP 515 – 565 nm).

2.4.2 Whole-Cell Patch-Clamp Recordings

Membrane currents were recorded in the fast whole-cell mode of the patch-clamp technique as was described previously (Shimizu T. et al. 2006; Wehner F. et al. 2003) at room temperature (22 – 26 ^{o}C). The patch electrodes were fabricated from borosilicate glass capillaries (Harvard Apparatus LTD, Edenbridge, UK) using a DMZ-Universal Puller (Zeitz-Instrumente Vertriebs GmbH, München) and had resistances close to 2.5 MΩ. Pipettes were positioned by use of motorized micro-manipulator (Luig and Neumann, Ratingen) and an Ag-AgCl wire served as the reference electrode. Pipette offsets, series resistance, and capacitive transients were compensated for on the patch-clamp amplifier (Axopatch 200A; Molecular Devices, Union City, CA). Data acquisition and analysis were done with the pCLAMP 8.0 software (Molecular Devices). The same software was used for the computation of liquid junction potentials of pipettes that were compensated for. Currents were filtered at 1 kHz and digitized with an AD converter (DigiData 1200B; Molecular Devices) at 5 kHz. Holding voltage was -30 mV, and voltage ramps from -80 to +20 mV and 1 sec duration were applied every 10 sec.

The pipette solution (pH 7.3) contained (in mmol/l): NaCl, 26; Na-gluconate, 69; $MgCl_2$, 1; TEA-Cl, 2; Na_2-ATP, 2; Na_2-GTP, 0.5; HEPES, 10; EGTA, 1. Osmolality was adjusted to 300 mosmol/kg-H_2O by addition of mannitol under osmometric control (OM802; Vogel, Giessen, Germany). The bath solution (pH 7.5) contained (in mmol/l): NaCl, 94; Na-gluconate, 6; $MgCl_2$, 1; $CaCl_2$, 1; TEA-Cl, 2; HEPES, 10. Osmolality was adjusted to 340 (isotonic) and 450 mosmol/kg-H_2O (hypertonic). With the above ion gradients, the equilibrium potential for Na^+ and Cl^- (as the only permeant ions) was set at 0 and -30 mV, respectively, according to the Nernst equation:

$$V = \frac{RT}{zF} \ln \frac{Co}{Ci}$$

where V is the equilibrium potential and Co and Ci are the outside and inside ion concentrations, respectively; R, T, F and z have their usual meaning.

Na$^+$ and Cl$^-$ conductances were calculated from the currents at -30 and 0 mV, respectively.

2.4.3 Pharmacology of the HICC

To inhibit the hypertonicity-induced non-selective cation current the following compounds were used: amiloride hydrochloride, flufenamic acid and gadolinium (III) chloride hexahydrate (Sigma Aldrich, Taufkirchen). The concentrations used for each inhibitor were 30, 50, 100, and 300µM. The stock solutions were prepared in DMSO (flufenamate and gadolinium) and ultrapure water (amiloride) according to the manufacturer's instructions, and then dissolved in the hypertonic bath solution (2.4.2) to the appropriate concentration. Compounds were applied following the maximum activation of the HICC current.

2.5 Scanning Acoustic Microscopy (SAM)

HepG2 cells were grown at low density on glass cover slips covered with collagen. The composition of isotonic and hypertonic bath solutions were the same as in the patch-clamp experiments (2.4.2) with osmolarity set as 300 mosmol/l and 410 mosmol/l, respectively.

Measurements of cell volume were performed continuously every minute during 10' under isotonic conditions, 10' under hypertonic conditions, and again 10' under isotonic conditions by Scanning Acoustic Microscopy. The cells transfected with siRNA were chosen by fluorescent signal from Alexa Fluor 488.

The experimental chamber (400 µl volume) was placed on the stage of an inverted microscope (Axiovert 10, Zeiss, Jena) and perfused by micropumps (Bartels Microtechnique GmbH, Dortmund) at a rate of ~ 1.2 ml/min. The temperature of the perfusate was kept at 37°C with the help of Peltier elements. 1 ns electrical impulse was converted into the acoustic signal of 1 GHz by use of a piezo element. The acoustic wave went through the sapphire lens and was focused on the cell surface. Acoustic signal was reflected by the glass substrate and partially by the cell surface. Then both signals went back through the lens to the piezoelectric transducer and were converted back into an electrical impulse (Figure 2.1) (Plettenberg S., 2007).

By use of the program SASAM Acoustic Investigator the time difference between signal E1 (from the cell surface) and signal E2 (from the glass substrate) was calculated and converted into the cell height. 2,500 measure points with size 2µm x 2µm were made at the scanned area of 100µm x 100µm. To increase the signal-to-noise ratio, the software subtracts the static noise of the lens.

Data analysis and cell volume calculations were made by use of the SASAM Acoustic Researcher software.
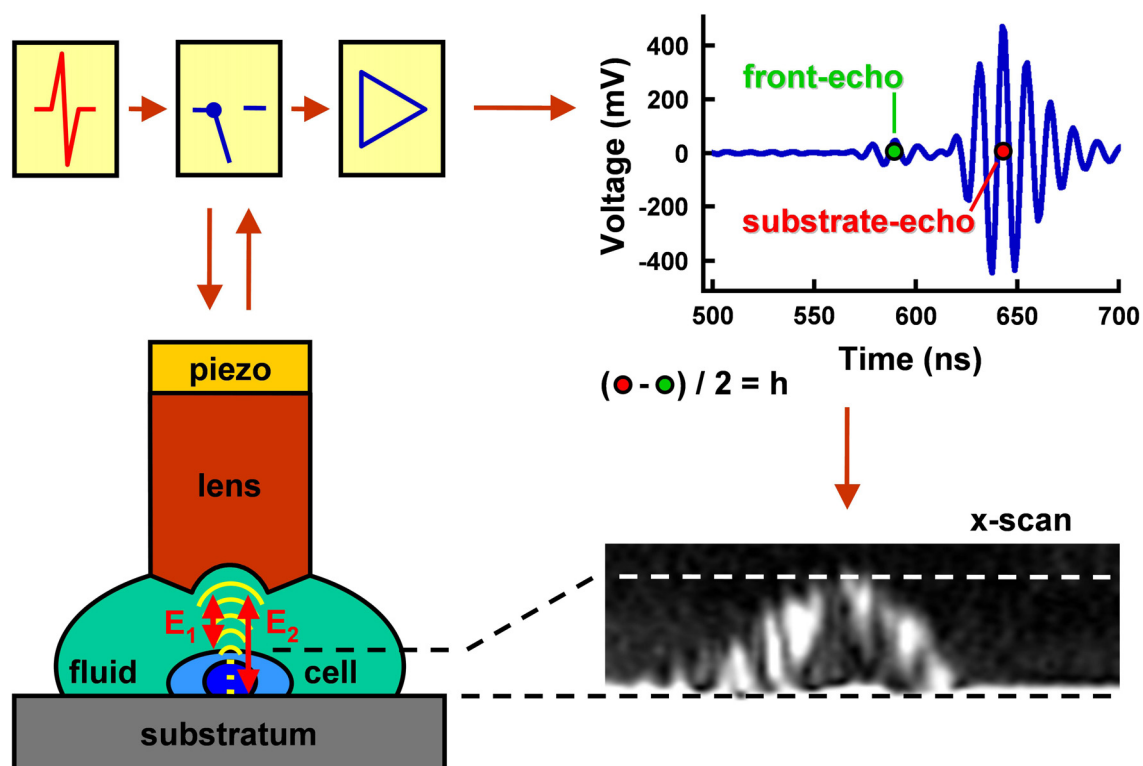
Figure 2.1: SAM. The principle of the technique. A 1-GHz sound wave is generated with a piezo-element and focused on the cell through a sapphire lens. In the lower right, a scan of a single cell in a single dimension (x-scan) is exemplified.

2.6 Measurement of Cell Proliferation

2.6.1 MTT Test

HepG2 cells (10,000 cells/well) were cultured in plastic 96-well culture plates with total volume of 200 µl growth medium per well. They were cultured under the control conditions and in the presence of increasing concentrations of amiloride and flufenamate (30, 50, 100, and 300 µM), or following transfection with siRNA against α-ENaC. Both treatment and control groups were performed in 8 replicate wells. After 24-hours incubation, the number of viable cells was determined by addition of 1 mg/ml of 3-[4,5-dimethylthiazol-2-yl]-2,5-diphenyl tetrazolium bromide (MTT) for 2 hours. Live cells assimilate MTT, which results in the accumulation of formazan crystals. These were then solubilized with acid isopropanol (90% isopropyl alcohol, 25% HCl) for 1 hour. The optical density of this solution measured at 550 nm (DYNATECH MR5000) is directly related to the number of live cell. These experiments were repeated at least six times.

2.6.2 Vi-Cell Counting

HepG2 cells (2×10^5 cells/well) were cultured in plastic 12-well culture plates with a total of 2 ml of growth medium. They were cultured under control conditions and in the presence of increasing concentrations of amiloride and flufenamate (30, 50, 100, and 300 µM), or following transfection with α-ENaC siRNA. Both treatment and control groups were performed in 3 replicate wells.

The numbers of viable and dead cells were then determined after 24-hour incubation by trypsinisation and counting by use of Cell viability analyzer (Vi-CELL^{TM} XR, Beckman Coulter, Fullerton, CA, USA), based on trypan blue exclusion. These experiments were repeated at least six times. Proliferation was calculated as a difference between the cell number before addition of drugs and cell number after 24 hours incubation with drugs.

2.7 Cell Cycle Analysis

2.7.1 DNA Staining

HepG2 cells ($2x10^5$ cells/well) were cultured in plastic 12-well culture plates with a total of 2 ml of growth medium. 26 hours after transfection with the siRNA, cells were trypsinised and washed with ice cold PBS. After fixation (2 % paraformaldehyde (PFA) in PBS, 10' on ice) and permeabilization (0,25 % Triton X-100 in PBS, 5' on ice), cells were stained with Hoechst 33258 (Sigma-Aldrich) (1,2 µg/ml in PBS, 20' at 37 ^{o}C) and subjected directly to the measurement.

2.7.2 FACS Analysis

Analysis was performed on a three-laser Becton Dickinson LSR II Flow Cytometer (BD Bioscience, Heidelberg) using the VioFlame Plus violet laser (25 mW, 405 nm) and the Sapphire blue laser (20 mW, 488 nm). Excitation and

emission settings were as follows: 405 nm excitation and 440/40 band pass filter for Hoechst; 488 nm and 530/30 band pass filter for Alexa Flour 488. The LSR II was driven by BD FACSDiva software with features such as reusable acquisition templates, automated compensation, and offline compensation.

2.7.3 FACS Data Analysis

The data from FACS analysis were analyzed by use of the FlowJo software (Tree Star, OR, USA). To derive cell cycle fractions G1/G0, S and G2/M from DNA histograms, we followed the method described by Stal & Baldetorp (1998; also Baldetorp B. et al., 1998). Special care was taken to include only single cells in our analysis and to exclude G0/1 doublets, which were discriminated using pulse height vs. pulse area of the Hoechst signal (Wersto R. P. et al., 2001). For all flow cytometric results reported, at least 50,000 cells were analysed and, in most instances, the number of cells was in the range of 70,000 and 100,000.

2.8 Cell Sorting

HepG2 cells transfected with siRNA conjugated with Alexa Fluor 488 were sorted on the FACS DiVa high-speed cell sorter (Beckton Dickinson, Heidelberg) at 488nm (Argon, Blue). The confirmed sample purity was more then 90 %.

Sorted cells (around 10^6 per sample) were lysed in an ice-cold lysis buffer (10% glycerol, 50 mM Tris-HCl pH 7.4, 100 mM NaCl, 1% Nonidet P-40, 2 mM

MgCl2, 100 µM PMSF, 1 mM bezamidine, 1 µg/ml leupeptin, 7 µg/ml pepstatin A). Debris were removed by centrifugation at 41 000×g for 30 min. The protein concentration of the supernatant was determined by the Bradford method, adjustment to an identical value in all samples occurred by addition of lysis buffer. After addition of 5xSDS sample buffer all probes were subjected to SDS-PAGE followed by Western Blot (2.3.2, 2.3.3).

2.9 Statistical Analysis

Mean values ± s.e.m. are presented, with n denoting the number of separate experiments performed. Significance was determined by paired and unpaired student's t tests. P values ≤ 0.05 were considered significant and denoted with * for $p \leq 0.05$, ** for $p \leq 0.01$, and *** for $p \leq 0.001$.

2.10 Primers and Antibodies

Table 2.1: Oligonucleotides used for sequencing, cloning and polymerase chain reactions

Primer name	Sequence (5`→ 3`)
Sequencing primers	
HumalphaENaC-279F	CACCTTTGGCATGATGTACTG
HumalphaENaC-299R	CAGTACATC ATGCCAAAGGTG
HumalphaENaC-677F	TCCAGCTGTGCAACCAGAAC
HumalphaENaC-1001F	CAGAGCAGAATGACTTCATTC
HumalphaENaC-1317F	CCAGAACGTGGAGTACTGTGAC
HumalphaENaC-1729F	CTGGTCATCATGTTCCTCATG
Cloning primers	
NheIHaENaC-1F	CTAGCTAGCGATGGAGGGGAACAAGCTGGAGGAG
HaENaC-HindIII-2010R	CCCAAGCTTTCAGGGCCCCCCCAGAGGAC
Mutagenesis primers	
FlagHumENaC-F	GTACAAATACAGCTCCTTCACCGACTACAAGGACGAC GACGACAAGCGCAGCCGTCGCGACCTGCG
FlagHumENaC-R	CGCAGGTCGCGACGGCTGCGCTTGTCGTCGTCGTCCT TGTAGTCG
HisHumENaC-F	GTACAAATACAGCTCCTTCACCCATCACCATCACCATC ACCGCAGCCGTCGCGACCTGCG
HisHumENAC-R	CGCAGGTCGCGACGGCTGCGGTGATGGTGATGGTGAT GGGTGAAGGAGCTGTATTTGTAC
PCR primers	
Human-β-actin1F	CTCGTCGTCGACAACGGCTC
Human-β-actin1R	AGTGGTACGGCCAGAGGCG
Human-αENaC1F	CAATGACAAGAACAACTCC
Human-αENaC1R	CCACCATCATCCATAAAG

RT-PCR primers	
Human-β-actin2F	CTGGCACCCAGCACAATG
Human-β-actin2R	GCCGATCCACACGGAGTA
Human-αENaC2F	CTGTGCAACCAGAACAAATCG
Human-αENaC2R	CAGCCTCCACAGGATGTTGA

Table 2.2: List of employed antibodies

Antibody	Comments
anti-α-ENaC	Monoclonal antibody from rabbit against human α-ENaC protein, diluted 1:1000 in Western blots, Sigma-Aldrich (Taufkirchen)
anti-β-ENaC	Monoclonal antibody from rabbit against human β-ENaC protein, diluted 1:1000 in Western blots, Sigma-Aldrich (Taufkirchen)
anti-γ-ENaC	Monoclonal antibody from rabbit against human γ-ENaC protein, diluted 1:1000 in Western blots, Sigma-Aldrich (Taufkirchen)
anti-δ-ENaC	Polyclonal antibody from rabbit against human δ-ENaC protein, diluted 1:100 in Western blots, Chemicon International (USA)
anti-CFTR	Monoclonal antibody from rabbit against human CFTR protein, diluted 1:1000 in Western blots, Sigma-Aldrich (Taufkirchen)
anti-ASIC1	Monoclonal antibody from rabbit against human α-ENaC protein, diluted 1:200 in Western blots, Sigma-Aldrich (Taufkirchen)
anti-TRPM7	Polyclonal antibody from rabbit against human TRPM7 protein, diluted 1:200 in Western blots, Chemicon international (USA)
anti-polycystin-2	Monoclonal antibody from mouse against human polycystin-2 protein, diluted 1:200 in Western blots, Santa Cruz Biotechnology (USA)
anti-rabbit	Polyclonal antibody from goat against rabbit IgG (H + L), HRP-conjugated secondary antibody for Western blotting (1:10000), Sigma-Aldrich (Taufkirchen)

anti-mouse	Polyclonal antibody from goat against mouse IgG (H + L), HRP-conjugated secondary antibody for Western blotting (1:10000), Sigma-Aldrich (Taufkirchen)

3. Results

## 3.1 HICC Activation and HepG2 Cell Proliferation

In primary human hepatocytes as well as in HepG2 cells, hypertonic cell shrinkage induced a non-selective cation conductance (Li T. et al., 2005; Wehner F. et al., 2002). In order to test for the putative correlation between HICC currents and proliferation in HepG2 cells, whole-cell patch-clamp experiments were performed.

3.1.1 Activation of Hypertonicity-Induced Cation Current in HepG2 cells

In whole-cell recordings on single HepG2 cells, hypertonic stress (+ 110 mosmol/l mannitol) led to a significant increase of membrane currents within a time range 5-15 min.

Figure 3.1.A depicts the Na^+ current obtained at E_{Cl} = -30 mV and the Cl^- current obtained at E_{Na} = 0 mV. At E_{Cl} = -30 mV, Na^+ conductance equaled 0.8 ± 0.1 and 6.5 ± 0.4 nS (p < 0.001) at times 2 and 8 min (see Figure 3.1.A), respectively. Cl^- conductance (at E_{Na} = 0 mV) was 0.2 ± 0.1 and 1.9 ± 0.1 nS (p < 0.001) at times 2 and 8 min (Figure 3.1.A). In most of cases the HICC activation

was almost completely reversible. Under isotonic and hypertonic conditions Zero-current voltages were -8.3 ± 1.7 and -6.0 ± 1.0 mV (n = 10, n.s.), respectively.
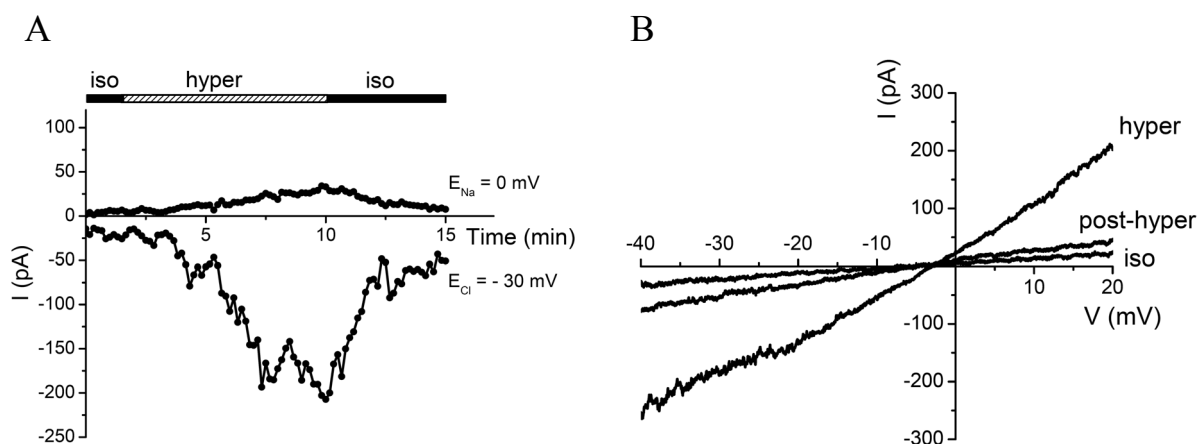
Figure 3.1: Effects of hypertonic stress on the membrane currents of a single HepG2 cell: (A) whole-cell currents at E_{Na} and E_{Cl}, as indicated; (B) complete current-to-voltage relations determined at min 2 and 8 (in A). Representative experiment.

3.1.2 Inhibition of HICC Currents

In previous studies, it was demonstrated that HICC activation in primary human hepatocytes and HepG2 cells is inhibited by amiloride, flufenamate and Gd^{3+} (Li T. et al, 2005., Wehner F. et al, 2002). To examine the dose-dependent inhibition of hypertonicity-induced cation currents, increasing concentrations of amiloride, flufenamate, and gadolinium were applied at the point of their maximum activation. Figure 3.2 exemplifies an experiment in which the effect of (300 µM) flufenamate on HICC currents was examined. The mean inhibition time was 4.0 ± 0.2 minutes for amiloride, 5.7 ± 1.1 minutes for flufenamate, and 4.9 ± 0.6 minutes in case of gadolinium.
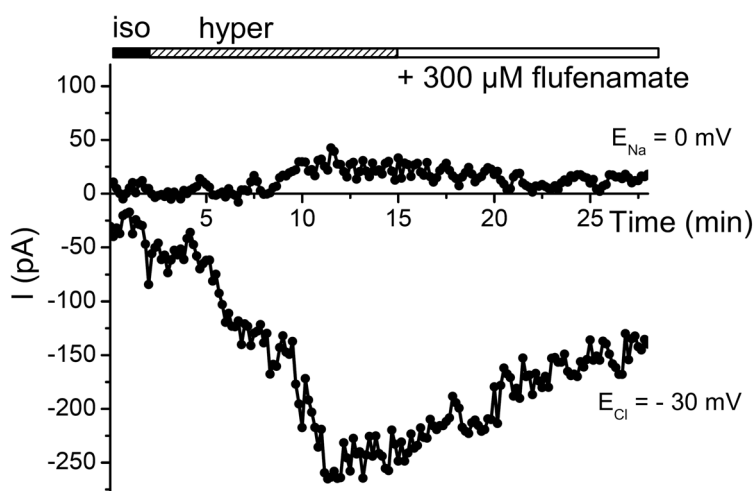
Figure 3.2: Inhibition of HICC current with 300 µM Flufenamate
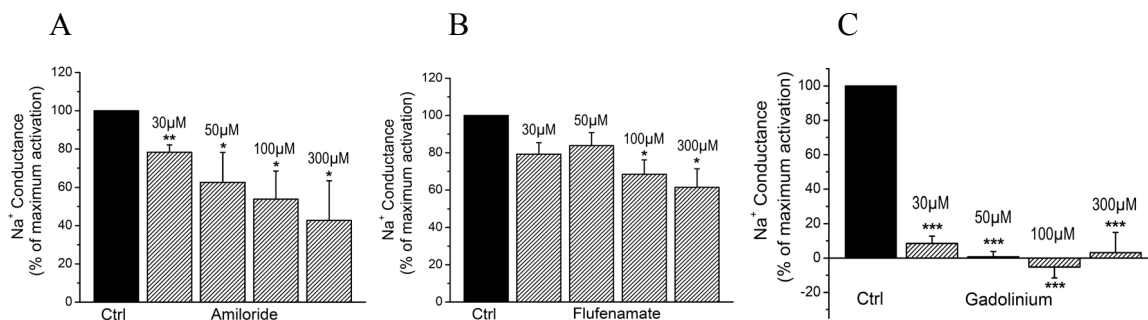
Figure 3.3: Concentration-dependence of the HICC inhibition by amiloride (A), flufenamate (B), and Gd^{3+} (C). Summary of currents at -30 mV (= E_{Cl}) with reference to the hypertonic control.

The complete inhibitory profile of HICC current is summarized in Figure 3.3. As is obvious from the figure, the HICC was inhibited by amiloride in a dose-dependent manner: with the hypertonic control activation taken as 100 %, currents at 30 µM amounted to 78.3 ± 3.8 % (p < 0.01), at 50 µM to 62.6 ± 15.6 % (p < 0,05), at 100 µM to 53.8 ± 14.7 % (p < 0.05), at 300 µM to 42.7 ± 20.6 % (p <

0.05) inhibition (n = 3-4). HICC inhibition by flufenamate was somewhat weaker with 79.2 ± 6.2 % (n.s.), 83.8 ± 7.0 % (n.s.), 68.4 ± 7.7 % ($p < 0.05$), and 61.4 ± 9.9 % ($p < 0.05$) at 30, 50, 100, and 300 µM respectively. Gadolinium appeared to be the strongest inhibitor of the HICC with 8.5 ± 4.3 % ($p < 0.001$), 0.8 ± 3.1 % ($p < 0.001$), -5.2 ± 6.4 % ($p < 0.001$), and 3.1 ± 1.9 % ($p < 0.001$) current inhibition at 30, 50, 100, and 300 µM respectively (n = 3-4). Nevertheless, no clear dose-dependency could be observed for this blocker.

3.1.3 Proliferation of HepG2 Cells

In order to test for the role of hypertonicity-induced cation channels in cell proliferation, the above data were taken as reference. HepG2 is a cell line with a high proliferation rate, and usually at 40 – 50 % confluency they double their number every 24 hours (data not shown). Different concentrations of amiloride and flufenamate were tested for the influence on HepG2 cell proliferation. It was not possible to use gadolinium in these measurements because some essential anions (phosphate, bicarbonate, sulfate) necessary for cell culturing avidly bind free Gd^{3+} and effectively remove it from solution (Ray A. et al, 1998).

Proliferation was measured by two independent methods: the MTT assay and Vi-CELL counting.
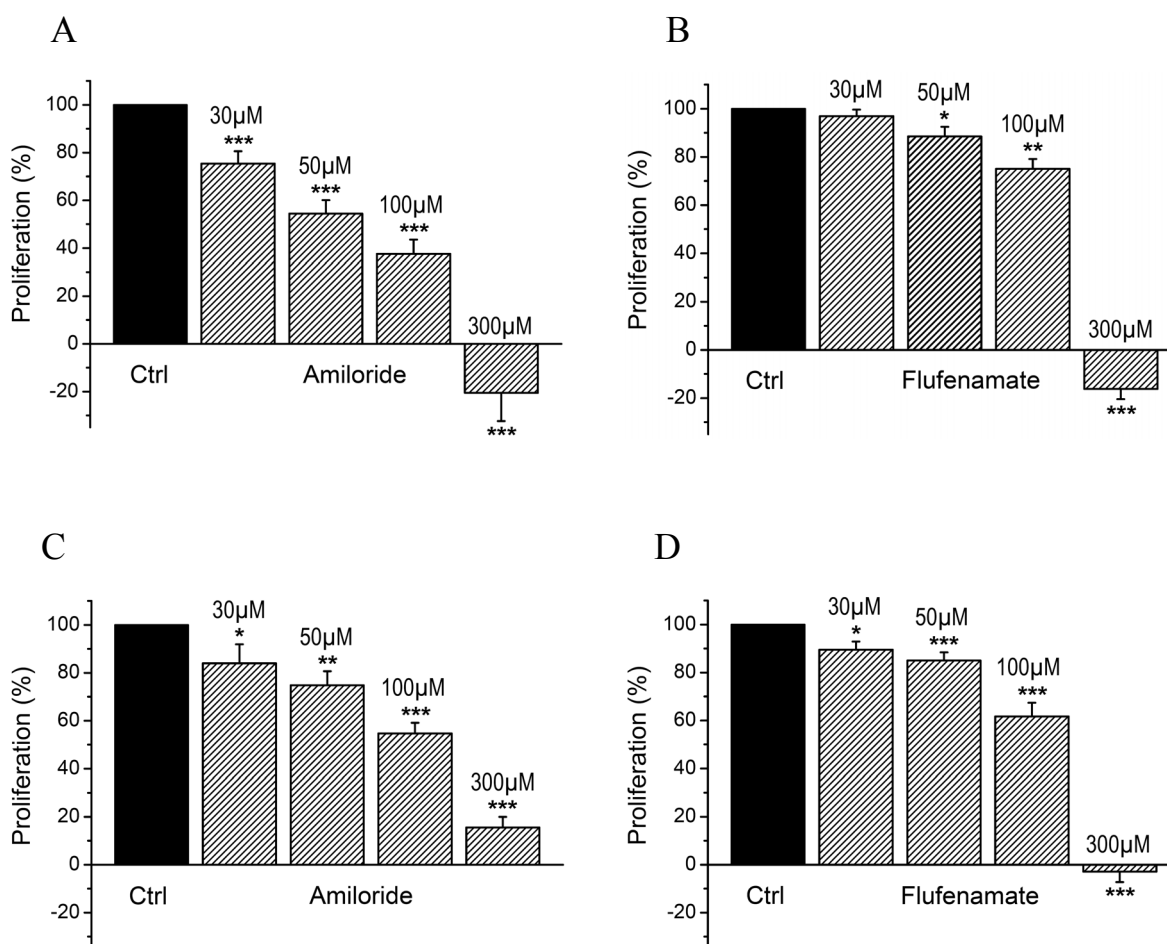
Figure 3.4: Concentration-dependent inhibition of HepG2 cell proliferation by amiloride (A, C) and flufenamate (B, D). MTT test (A, B) and Vi-CELL counting (C, D) were used to examine cell proliferation.

The inhibition of HepG2 cell proliferation with amiloride and flufenamate is depicted in Figure 3.4. It was found that HepG2 cells proliferation was sensitive to both compounds and that the effect was dose-dependently increasing. Application of the MTT method gave the following results: For amiloride: 30 μM led to 75 ± 5.2 % (p < 0.001) proliferation when compared with control, with 50 μM proliferation was 54.5 ± 5.6 % (p < 0.001), with 100 μM − 37.6 ± 5.9 % (p <

0.001), with 300 µM – -20.5 ± 11.8 % (p < 0.001) respectively (n = 7); For flufenamate: 30 µM led to 96.9 ± 2.7 % (n.s.) proliferation, 50 µM to 88.5 ± 4.1 % (p < 0.05), 100 µM to 75.1 ± 4.1 % (p < 0.01), 300 µM to -16.2 ± 4.2 % (p < 0.001) (n = 6). The data from Vi-CELL counting look not very different from the MTT test: For amiloride: 30 µM led to 86.3 ± 6.8 % (p < 0.05) proliferation when compared with control, 50 µM to 72.8 ± 5.2 % (p < 0.01), 100 µM to 53.9 ± 3.7 % (p < 0.001), 300 µM to 14.8 ± 3.6 % (p < 0.001) (n = 6); For flufenamate: with 30 µM proliferation was 89.1 ± 2.8 % (p < 0.05), with 50 µM – 82.3 ± 4.0 % (p < 0.001), with 100 µM – 61.1 ± 4.6 % (p < 0.001), with 300 µM – -6.4 ± 5.1 % (p < 0.001) (n = 6). The percentage of dead cells in the samples was following: 9.0 ± 2.2 % under the control conditions, 13.8 ± 3.3 % (n.s.) at 30 µM of amiloride, 13.7 ± 4.0 % (n.s.) at 50 µM, 15.4 ± 4.7 % (n.s.) at 100 µM, and 18.8 ± 3.4 % (p < 0.05) at 300 µM of amiloride. For flufenamate: 16.4 ± 3.2 % (n.s.) at 30 µM, 16.4 ± 3.5 % (n.s.) at 50 µM, 19.8 ± 4.4 % (n.s.) at 100 µM, and 46.1 ± 6.1 % (p < 0.001) at 300 µM.

3.2 Molecular Identification of Hypertonicity-Induced Cation Channel

The absence of the highly specific cation channels inhibitors lead to the decision of using siRNA technique to stop the translation of the particular gene of interest into a protein. An advantage of siRNA is that, since it only targets the specific gene in question, it leaves all the other elements of the cell unaffected. RNA interference comes into play between the steps of transcription and

translation. siRNA is introduced into the cell and binds to and destroys its mRNA target.

3.2.1 Silencing of α-ENaC Protein in HepG2 Cells

3.2.1.1 Transfection of α-ENaC siRNA in HepG2 Cells

Amiloride sensitivity of the HICC suggests epithelial sodium channel to be its possible molecular correlate. As the α-subunit is present in all the types of ENaC reported so far, it was chosen as a molecular target for the selective knockdown in HepG2 cells. Accordingly, HepG2 cells were transfected with specific siRNA duplexes against α-ENaC, conjugated with Alexa Fluor 488.

A   B
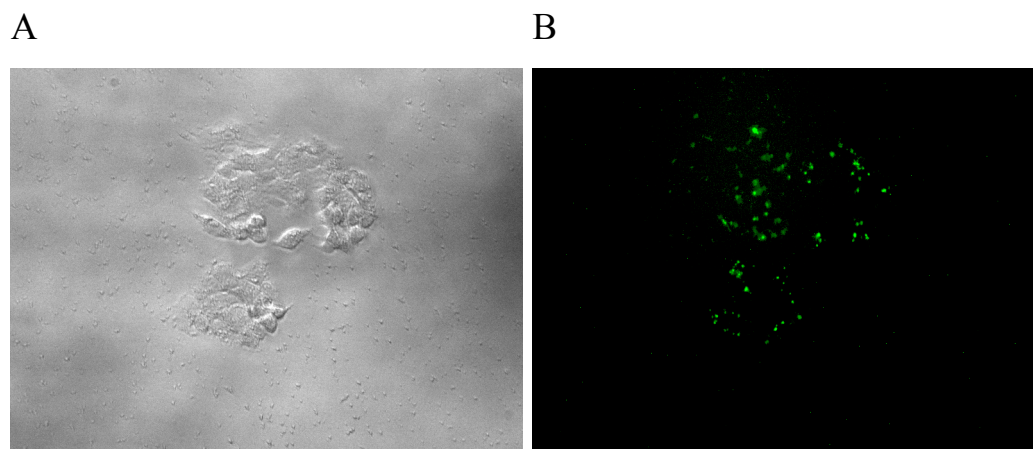
Figure 3.5: Transfection of HepG2 cells: phase contrast (A), green – fluorescence from siRNA (3`-Alexa Fluor 488) against α-ENaC (B).

The transfected cells could be easily differentiated from the non-transfected ones by the green fluorescent signal from siRNA. By estimation, about 50 % of the cells seem to contain siRNA duplexes. In addition, transfection efficiency was determined by FACS analysis. Usually, it varied between 40 and 60 % (data not shown).

3.2.1.2 Silencing of α-ENaC

The silencing effect of α-ENaC siRNA was confirmed by tree independent methods: polymerase chain reaction (PCR), real time quantitative PCR (RT-PCR), and Western blot analysis.

A mixture of transfected and non-transfected cells was used for both PCR experiments. It is quite clear from the Figure 3.6.I, that the amount of amplified α-ENaC fragments in siRNA transfected sample is remarkably reduced in comparison with the control with the equal amount of β-Actin in both samples. The experiment shown is representative of a total of three. Moreover, it was quantified by use of the real time PCR that there is only 40.5 ± 3.2 % ($p < 0.001$, n = 7) of α-ENaC mRNA left in the siRNA transfected HepG2 cells (Figure 3.6.II). Transfection efficiency varied from 40 to 60 % in these experiments (measured by FACS analysis).

Furthermore, Western blot analysis was performed to confirm the effect of α-ENaC siRNA on the protein level. As a first step, siRNA positive cells were sorted by the fluorescence activated cell sorter and the sample purity was more than 90 %. It is obvious from the Figure 3.6.III that amount of α-ENaC protein is

significantly reduced in the sample with siRNA positive cells although it is not completely removed. The experiment shown is representative of a total of three.

I

II

III
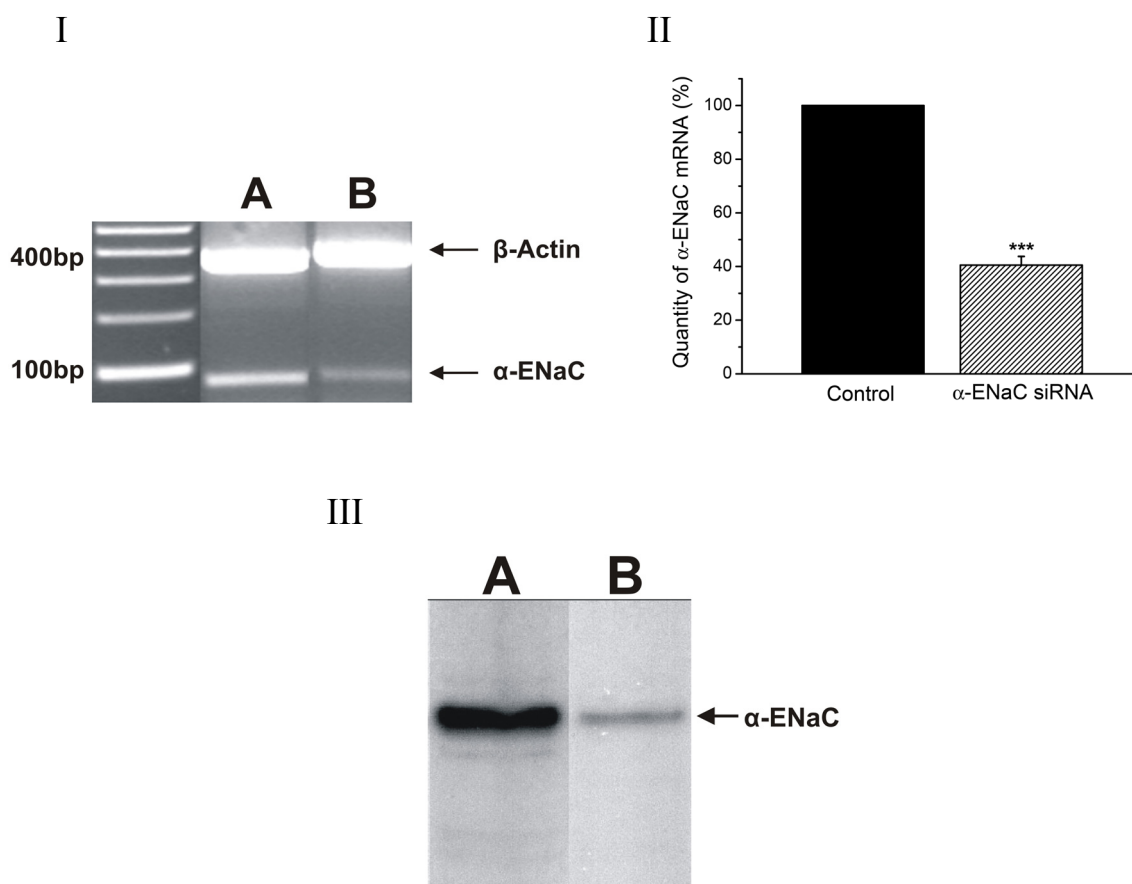
Figure 3.6.I: PCR analysis of α-ENaC in non-transfected control (A) and α-ENaC siRNA transfected (B) HepG2 cells. Agarose gel of the amplified α-ENaC and β-Actin fragments from cDNA after 35 PCR cycles is shown.

Figure 3.6.II: Quantitative real time PCR of α-ENaC in non-transfected and α-ENaC siRNA transfected HepG2 cells.

Figure 3.6.III: Western Blot analysis of α-ENaC expression in non-transfected control (A) and α-ENaC siRNA transfected (B) HepG2 cells. Transfected HepG2 cells were sorted by fluorescence-activated cell sorter.

3.2.2 α-ENaC and Na$^+$ Conductance in HepG2 Cells

To investigate the electrophysiological effect of α-ENaC silencing in HepG2 cells whole-cell patch-clamp recordings were performed. Transfected cells were selected from the fluorescent signal of the siRNA (conjugated with Alexa Fluor 488).

A   B
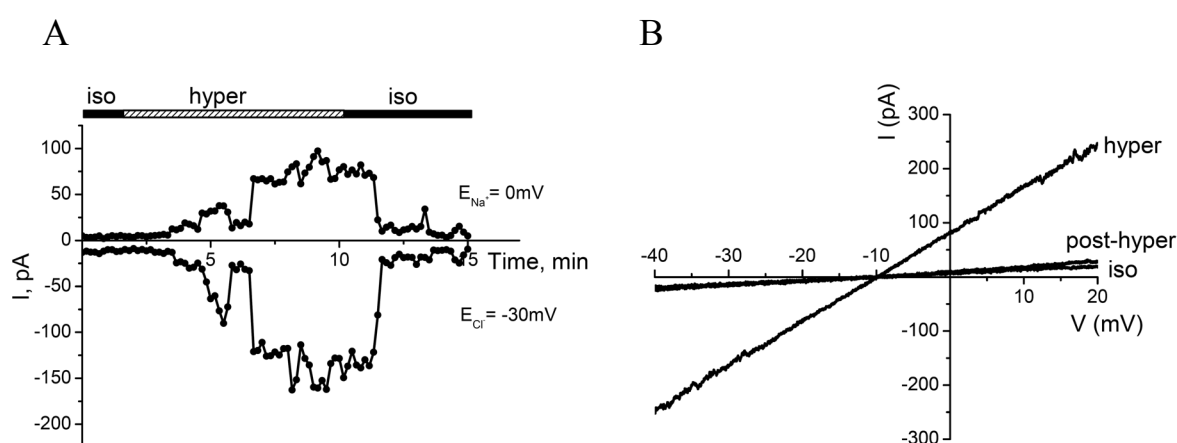
Figure 3.7: Effects of hypertonic stress on the membrane currents of a single HepG2 cell transfected with α-ENaC siRNA: (A) whole-cell currents at E_{Na} and E_{Cl}, as indicated; (B) complete current-to-voltage relations determined at min 2 and 8 min (A). Representative experiment.

Again hypertonic stress (+ 110 mosmol/l) led to a significant increase of membrane currents in 5-15 min and, at first sight, the complete current amplitude appeared to be not too different when compared to the control experiments. But the point of Zero-current voltage was always shifted to the left direction indicating the decrease of permeability for Na$^+$ and increase of Cl$^-$ permeability. The effect was present under both isotonic and hypertonic conditions.

Zero-current voltages were -14.7 ± 1.1 mV and -15.3 ± 0.8 mV (n = 14) under isotonic and hypertonic conditions respectively, which are both significantly different from the control experiments ($p < 0.01$, $p < 0.001$). Na^+ conductance equaled 0.4 ± 0.1 and 4.0 ± 0.4 nS ($p < 0.001$) at times 2 and 8 min (see Figure 3.7.A), respectively. Cl^- conductance amounted to 0.4 ± 0.1 and 4.7 ± 0.2 nS ($p < 0.001$) at times 2 and 8 min (Figure 3.7.A), respectively.

The values for the negative control siRNA were the following: Zero-current voltages were -7.9 ± 1.7 mV and -6.3 ± 1.7 mV under isotonic and hypertonic conditions (n = 6, $p > 0.05$), respectively. Na^+ conductance equaled 0.9 ± 0.2 and 6.4 ± 0.5 nS, Cl- conductance amounted to 0.2 ± 0.1 and 1.2 ± 0.4 nS under isotonic and hypertonic conditions, respectively.

The results from all the experiments are summarized in Figure 3.8. It is obvious that hypertonicity-induced as well as basal Na^+ permeability is remarkably decreased in HepG2 cells following α-ENaC silencing. In contrast, Cl^- permeability is significantly increased under these conditions.
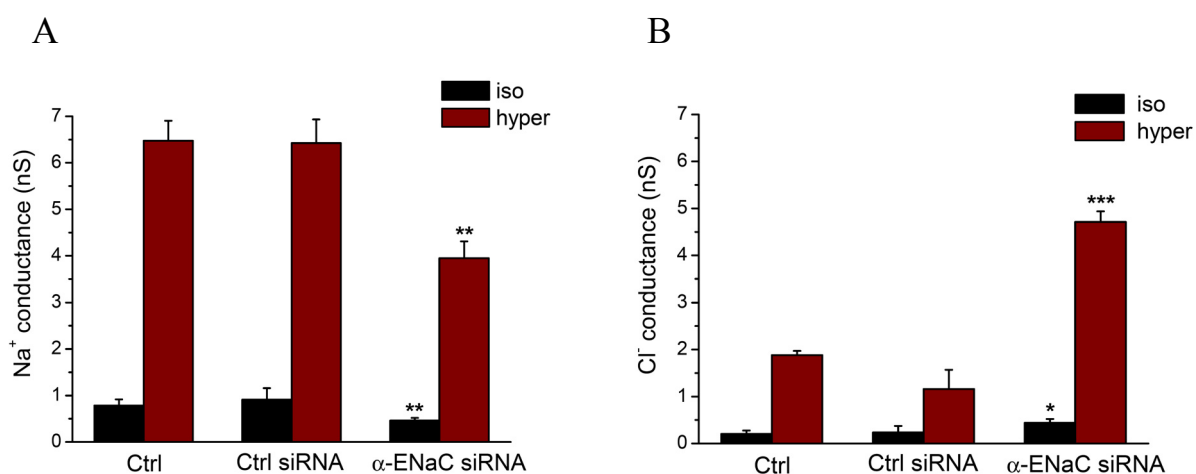
Figure 3.8: Na^+ (A) and Cl^- (B) conductance under iso- and hypertonic conditions, respectively.

3.2.3 α-ENaC and RVI in HepG2 Cells

After the role of α-ENaC in hypertonicity-induced membrane currents of HepG2 cells was established its actual role in cell volume regulation was of interest. Experiments were performed by the novel technique of time resolved acoustic microscopy. The major advantages of this method for cell volume measurement are the high accuracy, the absence of any radiation damage and photobleaching and the opportunity to use non-transparent samples and substrates (Weiss E. C. et al., 2007).

Experiments were done under control conditions, following treatment with transfection reagent, and with cells transfected with negative control siRNA and α-ENaC-siRNA. Under the isotonic conditions (300 mosmol/l), cell volumes equaled 2,83 ± 0,24 pl (n = 31) (Figure 3.9), 3,08 ± 0,41 pl (n = 6), 2,49 ± 0,20 pl (n = 13), and 3,01 ± 0,24 pl (n = 24) in control cells, in cells treated with transfection reagent, cells transfected with negative control siRNA, and cells transfected with α-ENaC-siRNA, respectively, which are not significantly different from each other. Increasing osmolarity from 300 to 410 mosmol/l, in the control experiments, led to a distinct shrinkage of HepG2 cells to 60.1 ± 2.8 % of initial volume within 2 min ($p < 0.001$, n = 31). Following this passive period of shrinkage, cells then partially regained their volumes, which, at 10 min of hypertonic stress, equaled 70.6 ± 2.6 % ($p < 0.001$) of control. With respect to the amount of cell shrinkage, this is equivalent to an RVI value of 26.4 ± 2.2 % ($p < 0.001$).
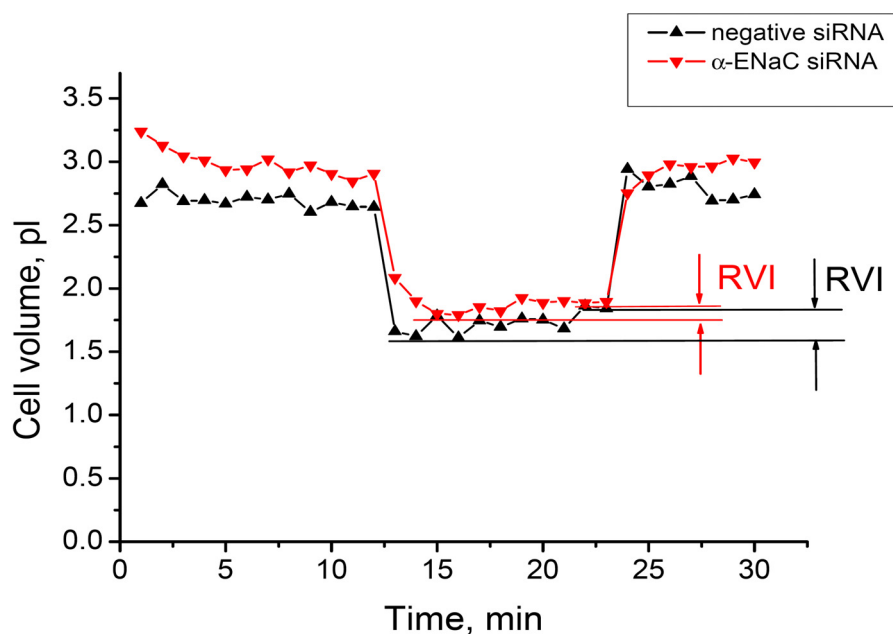
Figure 3.9: Hypertonicity-induced HepG2 cell shrinkage followed by RVI. The curve of a typical experiment from a cell transfected with negative control siRNA is shown in black, the curve of a typical experiment from a cell transfected with α-ENaC siRNA is shown in red.

The cells treated with transfection reagent and cells transfected with negative control siRNA showed a comparable RVI which was 25.4 ± 2.9 % (n.s.) and 28.8 ± 1.6 % (n.s.), respectively. In contrast, α-ENaC siRNA transfected cells had a significant reduction of RVI which equaled 8.3 ± 0.6 % (p < 0.001) (see Figure 3.10).

These experiments show that α-ENaC silencing reduced the RVI of HepG2 cells whereas the average cell size remained under isotonic control unchanged.
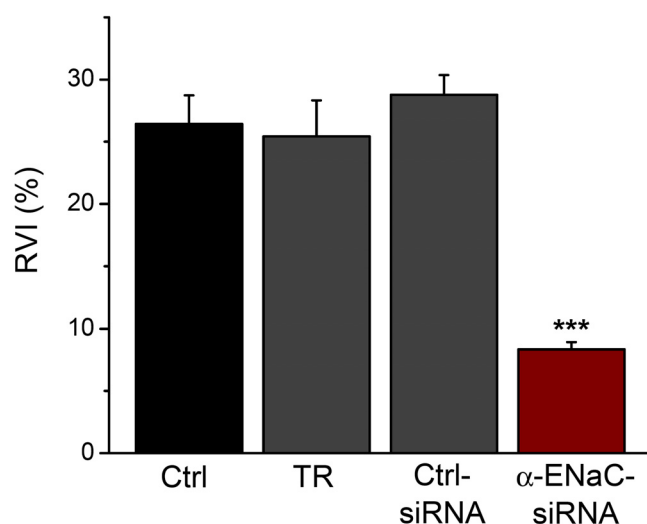
Figure 3.10: Effect of α-ENaC siRNA on the regulatory volume increase in HepG2 cells.

3.2.4 α-ENaC and HepG2 Cell Proliferation

The previous data (3.1.3) already suggest a role of the HICC in cell proliferation. To further test this working hypothesis siRNA technique in combination with proliferation assays were employed.

Figure 3.11 depicts the effect of α-ENaC silencing on HepG2 cell proliferation as it was determined by the MTT test and Vi-CELL counting. In both cases there is a small reduction of proliferation caused by transfection reagent, almost no effect of negative control siRNA, and a strong inhibition of proliferation in the sample with α-ENaC siRNA transfected cells (at a transfection efficiency was of 40 – 60 %).
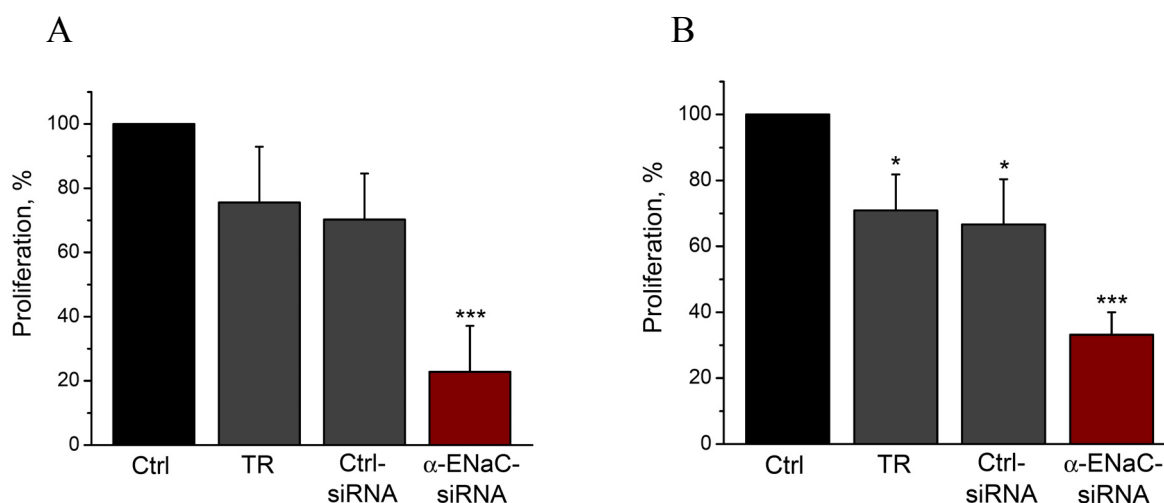
Figure 3.11: Effect of α-ENaC silencing on the HepG2 cell proliferation determined by MTT test (A) and Vi-CELL counting (B).

Proliferation calculated by MTT method equaled 75.5 ± 17.4 % (n.s.), 70.3 ± 14.4 % (n.s.), 22.8 ± 14.3 % (p < 0.001), with regard to 100 % control for the transfection reagent, negative control siRNA, and α-ENaC siRNA, respectively (n = 5). Application of the Vi-CELL counting gave the following results: 70.9 ± 10.9 % (p < 0.05), 66.6 ± 13.8 % (p < 0.05), 33.1 ± 6.8 % (p < 0.001) with regard to the control (100 %) for the transfection reagent, negative control siRNA, and α-ENaC siRNA, respectively (n = 6). The percentages of dead cells in the samples were following: 10.3 ± 1.6 % under the control conditions, 14.4 ± 1.6 % (n.s.) after the treatment with transfection reagent, 16.5 ± 2.4 % (p < 0.05) following transfection of the negative control siRNA, 17.9 ± 2.0 % (p < 0.01) following transfection of α-ENaC siRNA. The percentages of dead cells in samples with negative control and α-ENaC siRNA were not significantly different.

3.2.5 α-ENaC and the Cell Cycle of HepG2 Cells
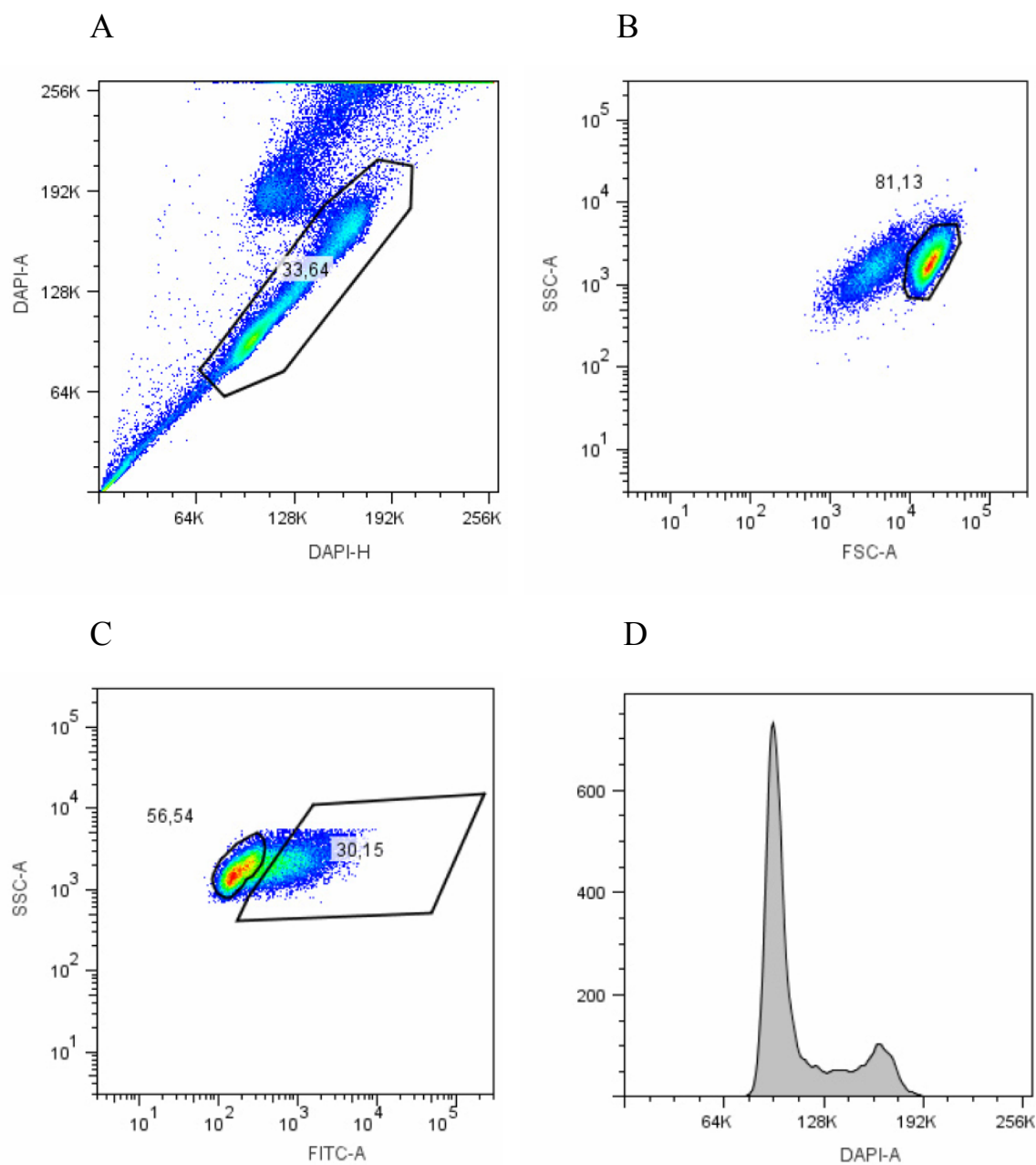
Figure 3.12: Algorithm of the FACS data analysis: definition of single cells (A), definition of living cells (B), separation of the Alexa 488 negative (left window) and positive (right window) cells (C), DNA analysis (D).

It was tempting to speculate that the strong inhibition of HepG2 cell proliferation by α-ENaC silencing may actually reflect changes in cell cycle distribution.

Phases of the cell cycle were evaluated with regard to the DNA content inside the cells by staining with Hoechst 33258. The cells transfected with siRNA were separated from the non-transfected ones with regard to the Alexa Flour 488 fluorescence. All collected data were analyzed in the following way (see figure 3.12): 1). single cells were separated from the doublets (Figure 3.12.A); 2). living cell were separated from the dead ones (Figure 3.12.B); 3). Alexa Fluor 488 containing cells were separated from the fluorescence negative cells if required (Figure 3.12.C); 4). DNA histogram of the chosen cell population which was analyzed by use of Dean-Jett-Fox model (Figure 3.12.D).
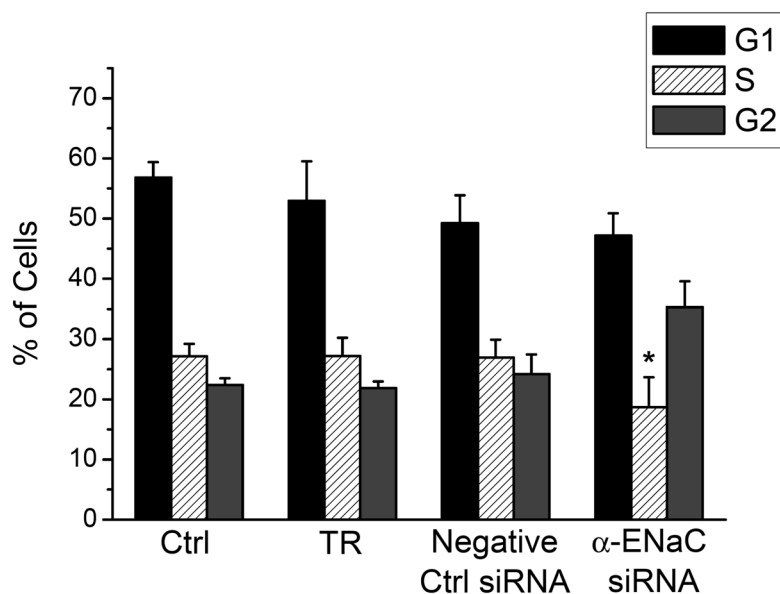
Figure 3.13: Effect of α-ENaC silencing on the HepG2 cell cycle.

The distribution of HepG2 cells over the cell cycle is depicted in Figure 3.13. Under control conditions G1, S, and G2 phases equaled 56.8 ± 2.6 %, 27.2 ± 2.1 %, and 22.4 ± 1.1 % respectively (n = 5). Treatment with transfection reagent didn't change this ratio significantly (52.9 ± 6.6 % (n.s.), 27.2 ± 3.0 % (n.s.), 21.9 ± 1.1 % (n.s.)). Also, introduction of the negative control siRNA caused only slight non-significant changes in the cell cycle distribution: 49.3 ± 4.6 % (n.s.), 26.9 ± 3.0 % (n.s.), 24.2 ± 3.3 % (n.s.) for G1, S, and G2 phase respectively. In contrast, silencing α-ENaC with siRNA resulted in the significant reduction of S phase and a tendency of an increase of G2 phase of the cell cycle: 47.2 ± 3.7 % (n.s.), 18.7 ± 4.9 % ($p < 0.05$), 35.3 ± 4.3 % ($p = 0.1$) for G1, S, and G2 phases respectively (n = 5).

3.2.6 Identification of the α-ENaC Interacting Proteins

In order to identify the proteins interacting with α-ENaC in HepG2 cells and, possibly, to define the overall architecture of the HICC, the following strategy was tried (see Figure 3.14): Tagged α-ENaC is overexpressed in HepG2 cells and chemically linked at the extracellular side to possible partners with a water-soluble DTSSP crosslinker. Then, after membrane isolation and protein solubilization, the protein complex is pulled down and digested with Trypsin for the following ESI-MS analysis or, it is eluted with the sample buffer for the following 1D or 2D-PAGE separation and MALDI-MS or Western Blot analysis.
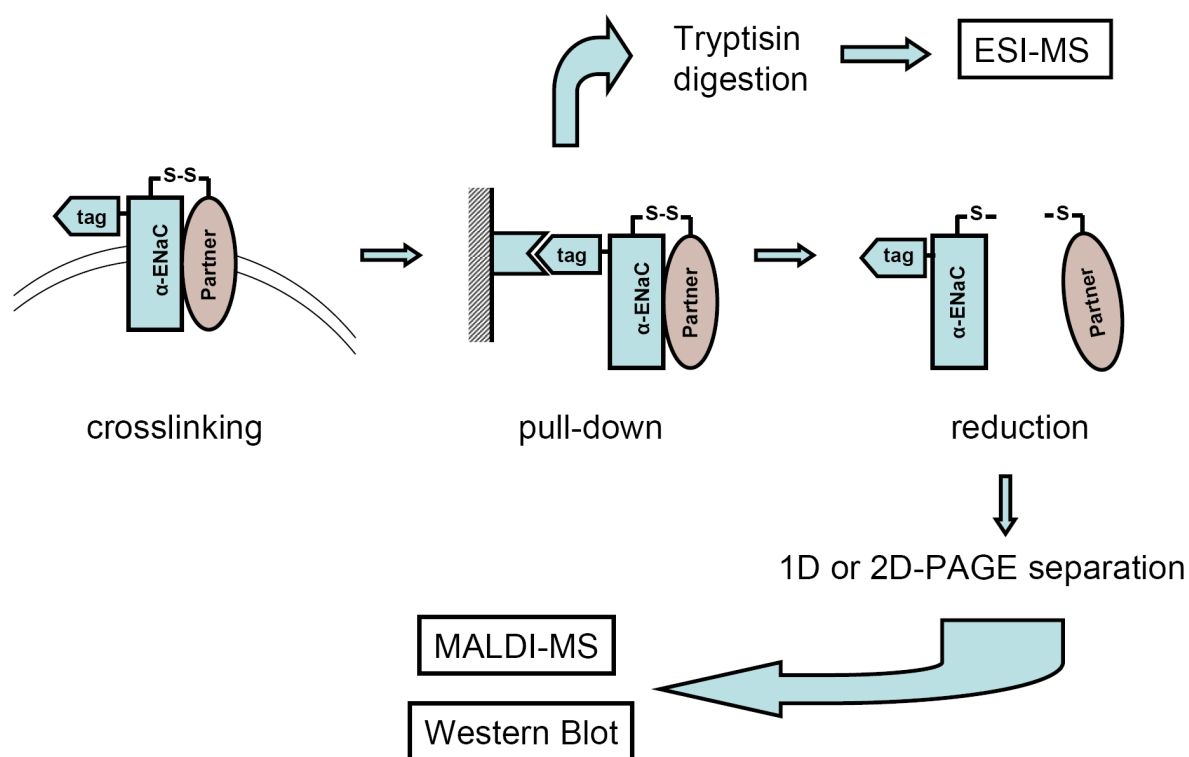
Figure 3.14: Experimental pathway for the identification of the α-ENaC interacting proteins.

3.2.6.1 Overexpression and Purification of the Tagged α-ENaC in HepG2 Cells

Overexpression of the tagged α-ENaC protein in stably transfected HepG2 cells was confirmed by Western Blot (Figure 3.15). Apparently, cell appearance and proliferation rate did not change under overexpression conditions. Nevertheless, α-ENaC protein expression seemed to be 8-10 times higher in transfected cells compared to the endogenous expression level (n = 3).
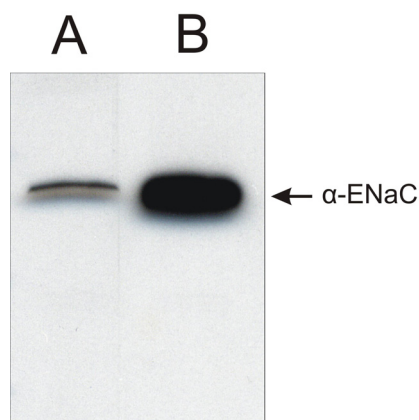
Figure 3.15: Western Blot analysis of α-ENaC expression in HepG2 cells: endogenous protein level (A), overexpression of α-ENaC in stably transfected HepG2 cells.

After the pull-down of the Flag-tagged α-ENaC, 1D gel electrophoresis was performed in order to separate it from the interacting proteins by molecular weight. Two samples with and without crosslinking step were prepared. The gel stained with Coomassie Blue is depicted in Figure 3.16. There are two bands of α-ENaC protein corresponding to 75 kDa and 87 kDa. The higher molecular weight band should correspond to the glycosylated form of α-ENaC (Dijkink L. et L., 2002; Hanwell D. et al., 2002). The lower band with ~ 50 kDa is likely to reflect the heavy chain of the anti-α-ENaC antibody. This appears to occur via the reducing agent present in the sample buffer used for elution. Obviously, there is no difference detectable between the samples with and without crosslinker.
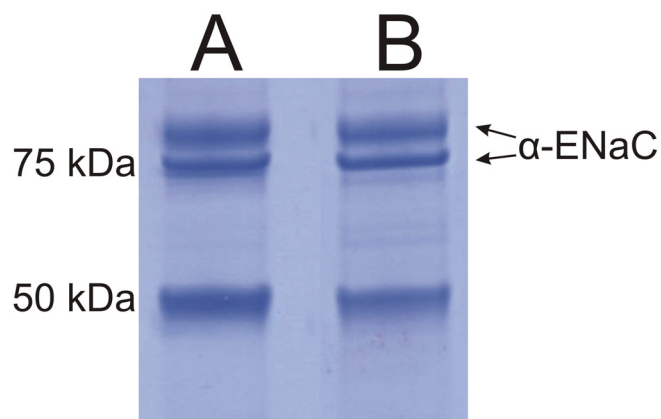
Figure 3.16. Coomassie staining of a 1D gel showing the purified Flag-tagged α-ENaC with (B) and without (A) DTSSP crosslinking.

In order to separate proteins interacting with α-ENaC on the basis of two parameters (isoelectric point and molecular weight) a two-dimensional gel electrophoresis was used. Again, two samples were prepared (with and without crosslinker) to check for additional protein spots appearing after crosslinking. The results of silver staining of gels are depicted in Figure 3.17.

Apparently, the gels are overloaded with α-ENaC protein (black arrows) and light and heavy chains of the anti-α-ENaC antibody (blue arrows). There are also some protein spots present in both gels which should correspond to the background proteins that bind to the resin during pull-down non-specifically. Nevertheless, only very minor changes are seen between two gels.
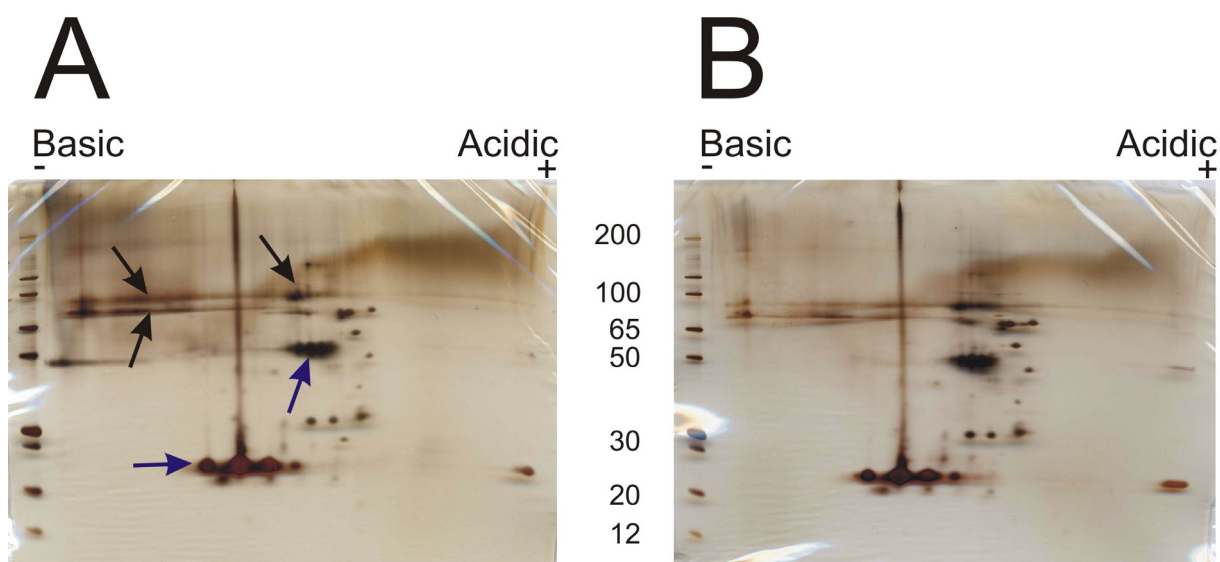
Figure 3.17: Silver staining of the 2D gels showing the purified Flag-tagged α-ENaC with (B) and without (A) DTSSP crosslinking.

3.2.6.2. Expression of α-, β-, γ-, δ-ENaC, CFTR and TPRM7 in HepG2 Cells

In order to check the expression of these putative candidates to interact with α-ENaC in HepG2 cells the Western blot technique was used. Protein samples were prepared from the whole cell lysates.

It was found that α-, γ-, and δ-, but not β-subunit of ENaC are expressed in HepG2 cells (Figure 3.18) (n = 4). The first bands of α-, γ-, and δ-subunits were detected at approximately 75 kDa. The second bands of γ- and δ-subunits (at approximately 85 – 90 kDa) should correspond to the glycosylated forms of the proteins (Dijkink L. et L., 2002; Hanwell D. et al., 2002). Surprisingly, the level of

γ-ENaC subunit seemed to be very high in comparison with α- and δ-ENaC subunits.
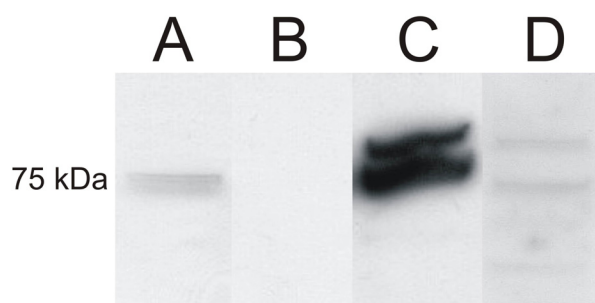
Figure 3.18: Western Blot analysis of α- (A), β- (B), γ- (C), and δ-ENaC subunits expression in HepG2 cells.
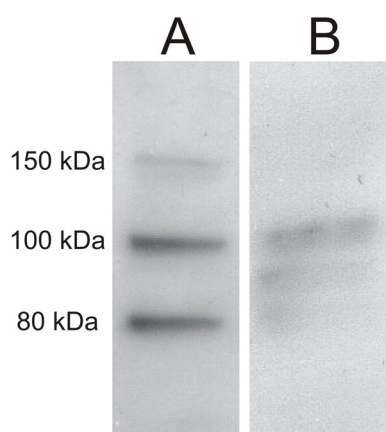
Figure 3.19: Western Blot analysis of CFTR (A) and TRPM7 (B) expression in HepG2 cells.

The cation channels TPRM7 and TRPP2 were chosen as the potent candidates to contribute to the HICC (1.3.4) in HepG2 cells. Also, acid sensitive ion channel (ASIC) was recently demonstrated to form intermolecular interactions with ENaC subunits (Meltzer R. H. et al., 2007). Besides, numerous reports show

the facts of physical protein-protein interaction of ENaC and cystic fibrosis transmembrane conductance regulator (CFTR) (Schwiebert E. M. et al., 1999; Reddy M. M. et al., 1999; Ji H.L. et al., 2000; Kunzelmann K., 2001). Thus, the expression of the listed proteins was tested in HepG2 cells.

There were no signals found for TRPP2 and ASIC1 channels in HepG2 cells (n = 2). CFTR protein was detected at 150, 100 and 80 kDa which correspond to the predicted molecular mass (n = 3). The bands observed with the antibody against TRPM7 protein were detected at 98 and 85 kDa, which have been never reported for this protein (n = 2).

4.Discussion

4.1 HICC Activation and HepG2 Cell Proliferation

In the present study, the hypertonicity-induced cation channel in human hepatocytes and its role in proliferation were investigated. HepG2 cells were chosen as a model to study the HICC properties and the interplay between RVI processes and proliferation in the same system.

4.1.1 The Hypertonicity-Induced Cation Current in HepG2 Cells

Under hypertonic stress, HepG2 cells demonstrated the activation of Na^+ inward currents. A similar observation was made in previous studies on HepG2 cells (Wehner F., Lawonn P., Tinel H., 2002) and in primary human hepatocytes (Li T. et al., 2005). The change in Zero-current voltage appears to be not significant what is not typical for the Na^+ currents. But it is quite obvious that Cl^- currents were activated in parallel with Na^+ and the time course of activation was very similar. This does explain the absence of any significant shift in reversal potential. Also of note, in this respect, the previous works on primary human hepatocytes demonstrated that the HICC currents are dependent on the

extracellular Cl^- concentrations (Li T. et al., 2005). This Cl^- sensitivity was interpreted in terms of a safety mechanism so that, under conditions of an outwardly directed Cl^- gradient, the activation of the non-selective cation channel may be too dangerous since it may lead to an actual overall release of osmolytes rather than to a net cellular uptake (Wehner F., 2006). Moreover, the HICC current was sensitive to the Cl^- channel blockers NPPB, SITS (Li T., Wehner F., unpublished observations). Taken together, this findings support the notion of an interplay of cation and anion conductance under hypertonic stress and during RVI.

Interestingly, activation of HICC current in HepG2 cells following hypertonic stress takes 5-15 minutes which is a factor of 2 to 3 slower when compared to the usual activation time. It should be taken into account, however, that cells were detached from their support prior to the experiments. Under these conditions, focal-adhesion signaling will be reduced which was shown to be an upstream event leading to channel activation and restoration of cell volume (Olsen H. et al., 2007).

4.1.2 Inhibition of HICC Current

The sensitivity of HICC currents in human hepatocytes to certain blockers had been already reported earlier. Amiloride, flufenamate and gadolinium were shown to inhibit the HICC in primary human hepatocytes as well as in HepG2 cells (Li T. et al, 2005., Wehner F. et al, 2002), although the dose-dependence of such an inhibition was not tested so far. Amiloride is an antikaliuretic-diuretic agent, which is known to block the epithelial sodium channel (ENaC) (Schild L. et al., 1997). Flufenamic acid (flufenamate) is a non-steroidal anti-inflammatory drug

which acts as a blocker of non-selective cation channels (Poronnik P. et al., 1992). Gadolinium (Gd^{3+}) is a classical blocker of the stretch-activated ion channels (Yang X. C. and Sachs F., 1989).

In the present study, it was found that the hypertonicity-induced cation conductance in HepG2 cells is inhibited by increasing concentrations of amiloride and flufenamate in a dose-dependent manner. The similar dose-dependent inhibition of HICC currents was recently reported for the human cervix carcinoma cell-line HeLa (Shimizu T. et al., 2006).

The strongest inhibitory effect was reached by Gd^{3+} what is in line with the observations on primary human hepatocytes (T. Li et al., 2005) and HepG2 cells (F. Wehner et al., 2002). Amiloride and flufenamate demonstrate the partial inhibition of the channel at 100 μM what was also observed in the previous studies (F. Wehner et al., 2002).

Just based on their pharmacology, one may distinguish a group of hypertonicity-induced cation channels that is inhibited by the diuretic amiloride (but that is insensitive to flufenamate) from one that is insensitive to amiloride (but efficiently blocked by Gd^{3+} and flufenamate) (Wehner F., 2006). Amiloride-sensitive cation channels were also shown to be activated by the hypertonic stress in confluent monolayers of rat hepatocytes (Wehner F. et al., 1995), U937 macrophages (Gamper N. et al., 2000), human red cell ghosts (Huber S. M., et al., 2001).

Amiloride-insensitive hypertonicity-induced cation channels are expressed in a variety of systems including human nasal epithelial cells (Chan HC and Nelson DJ, 1992), the colonic cell-lines CaCo-2 and HT29 (Nelson DJ et al., 1996; Koch JP and Korbmacher C., 1999), mouse collecting duct M1 cells (Volk T. et al., 1995) and HeLa cells (Wehner et al., 2003).

Interestingly, hypertonicity-induced cation channels with a combined pharmacology also exist and these may reflect a molecular link between the two groups reported so far. This type of channels is observed in primary human hepatocytes (Li T. et al., 2005), in HepG2 cells (Wehner F. et al., 2002), in mouse Ehrlich-Lettre-ascites (ELA) tumour cells (Lawonn P. et al., 2003).

4.1.3 HICC and Proliferation of HepG2 Cells

The increase of cell volume is apparently required for the initiation of cell proliferation. Moderate osmotic swelling has been shown to stimulate (Anbari K. and Schultz R.M., 1993) and osmotic shrinkage has been shown to inhibit (Higgins C. F. et al., 1987; Petronini P. G. et al., 1992) cell proliferation. Upon sustained exposure to hypertonic extracellular fluid the cells overcome cell shrinkage by cellular accumulation of osmolytes, which subsequently allows them to proliferate again (Lawitts J. A. and Biggers J. D., 1992; Yancey P. H. et al., 1990).

In the present study it was demonstrated that amiloride and flufenamate inhibit HICC current in HepG2 cells in a dose-dependent manner while Gd^{3+} blocks the channel at low concentrations completely. As HICC is a main player of RVI in human hepatocytes, we were wondering if the isotonic inhibition of this channel may have an effect on cell proliferation. And indeed, increasing concentrations of amiloride and flufenamate effectively inhibited proliferation of HepG2 cells in a dose-dependent way. The numerically negative proliferation values at 300 µM of amiloride and flufenamate measured by MTT method may be a result of the side effects caused by the high drug concentration. Accordingly, the amount of dead cells measured by Vi-CELL counting was 18.8 % and 46.1 % in

case of 300 µM amiloride and flufenamate, respectively (3.1.3). With regard to amiloride, the concentrations above 100 µM may also block Na^+/H^+ exchanger (Kleyman T. R. and Cragoe E. J., 1998) which is critical for the normal cell metabolism and also employed in cell proliferation (Bianchini L., Grinstein S., 1993; Ritter M., Wöll E., 1996).

Inhibition of proliferation exhibited pharmacological profiles that were very similar to those of the inhibition of the HICC. Considering these results, it appears that inhibition of HICC results in the reduction of proliferation in a given system and the channel is most likely the important player involved in the regulation of this process (see Figure 4.1).
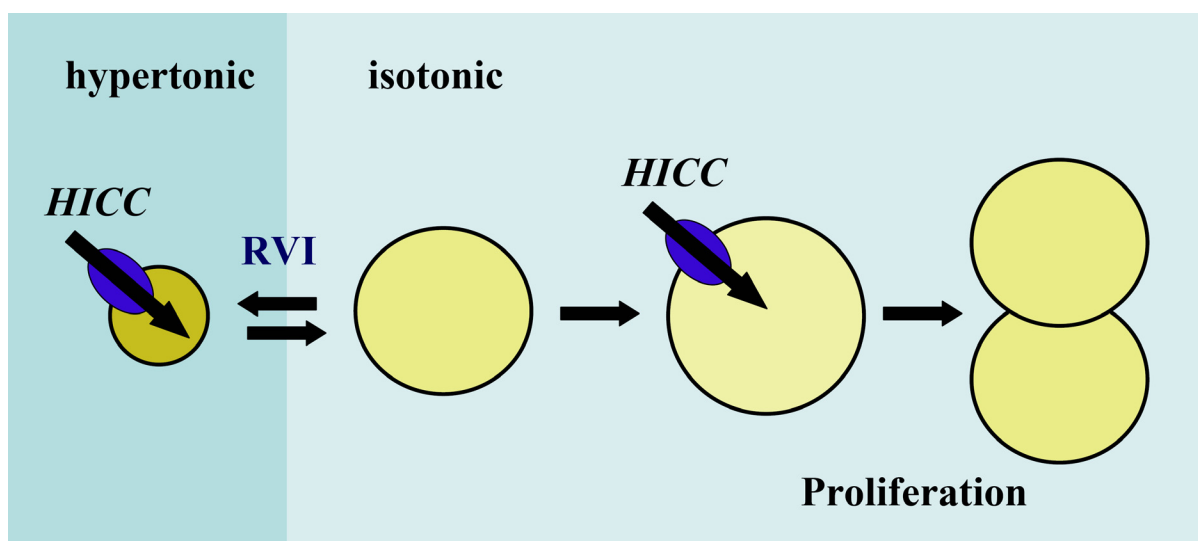
Figure 4.1: Possible interplay between hypertonicity-induced cation channels and HepG2 cell proliferation.

The similar results were recently obtained by Shimizu T. et al. (2006) for HeLa cells. The authors reported that with HICCs blocked by flufenamate and Gd^{3+} a significant reduction of proliferation and a stimulation of apoptosis were

observed. Both effects exhibited virtually identical sensitivity profiles to osmotic stress as well as to flufenamate and Gd^{3+}. Moreover, the observed concentration dependency of flufenamate and Gd^{3+} on proliferation and apoptosis was in excellent accordance with that on HICC inhibition.

Taking into account that Gd^{3+} avidly binds to anions commonly present in physiological salt solutions and culture media, including phosphate- and bicarbonate-buffered solutions (Caldwell R. A. et al., 1998), we decided not to use this ion in our experiments.

4.2 Molecular Identification of Hypertonicity-Induced Cation Channel

Evidence has been reported that the α-subunit of epithelial sodium channel is a possible molecular correlate of the HICC. Accordingly, application of siRNA directed against α-ENaC was considered as a useful tool to test for the actual contribution of ENaCs to HICCs and their role in proliferation.

Transfection of the siRNA duplexes in HepG2 cells led to the remarkable knock-down of the α-ENaC mRNA and protein levels. At the mRNA level the silencing effect of the siRNA was very close to 100 %. This conclusion comes from the comparison of the HepG2 transfection efficiency and the quantitative data got by real-time PCR. The α-ENaC protein level is also significantly reduced although the knock-down is not complete. The half-life of (heterologously expressed) ENaC at the cell surface of *X. laevis* oocytes after brefeldin A treatment was reported to be ~2–3.5 h (Shimkets R.A. et al., 1997; Staub O. et al., 1997). In

mammalian MDCK cells, this value was between 1 and 2 h (Hanwell D., 2002), which is quite comparable considering the higher temperature in which these cells are grown relative to that for *X. laevis* oocytes. A recent study using A6 cells proposed a much longer half-life of *x*ENaC and suggested that cell surface stability of α- and γ-ENaC (at least 24 h) is much greater than that of β-ENaC (6 h) (Weisz O. A. et al., 2000; Kleyman T. R. et al., 2001). It is presently difficult to understand, however, the discoordinate internalization of the ENaC chains and the suggestion that they may traffic to and from the plasma membrane independently, considering the various studies demonstrating that ENaC chains assemble very early in the ER. Thus most studies suggest that ENaC at the cell surface is turned over quite rapidly (Rotin D. et al., 2001).

4.2.1 α-ENaC and HICC Current in HepG2 Cells

After confirmation of a successful α-ENaC silencing in HepG2 cells the first thing to do was to carry out the investigation of HICC currents. As a result, isotonic as well as hypertonicity-induced Na^+ currents in HepG2 cells were significantly reduced. Reduction of the hypertonicity-induced Na^+ current under condition of α-ENaC knock-down is quite in line with our hypothesis and some previous works on primary rat hepatocytes. The first direct evidence for a role of the ENaC in cell volume regulation was reported by Böhmer C. and Wehner F., 2001. They injected specific antisense oligonucleotides directed against α-rENaC into single rat hepatocytes in confluent primary culture and found an inhibition of hypertonicity-induced Na^+ currents by 70 %. It was recently shown that all three subunits of ENaC are functionally related to RVI and HICC activation in primary

rat hepatocytes (Plettenberg S., 2006). From *Xenopus* oocytes expressing α-, β-, γ-rENaC, it was reported that hypertonic stress increased and hypotonic stress decreased amiloride-sensitive currents, respectively, and these effects coincided with a decrease of P_{Na}/P_K from 20 (under isotonic conditions) to values of 11 and 6 (Ji H. L. et al., 1998).

An interesting fact is the reduction of the basal Na^+ conductance in HepG2 cells under the α-ENaC silencing. It is known, however, that the epithelial sodium channel plays an important role in Na^+ homeostasis by determining the Na^+ transport rate in so-called end-organs such as the renal collecting duct, distal colon, salivary and sweat gland ducts. It also plays a major role in the maintenance of electrolyte and water homeostasis in all vertebrates. So it could be possible that ENaC mediates a physiological electrolyte uptake in human hepatocytes.

The surprising fact was the significant increase of both isotonic and hypertonic Cl^- conductance. It was already stressed previously that hypertonicity-induced cation channels require Cl^- ions for their activation and appear to be blocked by some Cl^- channel inhibitors. So it appears that the cellular response to the hypertonicity may require Cl^- channels. There are numerous reports about the role of Cl^- channels in cell volume regulation but most of them seem to be implicated in the hypotonic responses. The apparently most abundant form of hypotonicity-induced Cl^- channels belongs to a group that has been named VSOR (volume-sensitive outwardly-rectifying) Cl^- channels (Okada Y., 1997), VRAC (for "volume-regulated anion channels" (Nilius B. and Droogmans G., 2001)), or VSOAC (volume-sensitive organic osmolytes-anion channels (Jackson P. S. et al., 1994)). Despite the rather ubiquitous presence of VSOR Cl^- channels, their molecular entity still remains a mystery. A possible molecular candidate is ICln, outwardly rectifying chloride channel when expressed in *Xenopus* oocytes

(Paulmichl M. et al., 1992). ClC-2 and ClC-3 were also considered as molecular candidates for VSOR Cl⁻ channels. ClC-2 is inwardly rectifying and is activated by strong hyperpolarizations, acidic extracellular pH, and cell swelling (Gründer S. et al., 1992). ClC-3 exhibits more similarities to VSOR Cl⁻ channels including outward rectification, unitary conductance, and ion selectivity (Hume J. R. et al., 2000). In most systems, hypotonic stress elicits a significant increase in cell Ca^{2+}. This in turn may lead to the activation of Ca^{2+}-dependent Cl⁻ channels (CaCCs) that may contribute significantly to the overall volume response (Hoffmann E. K. and Mills J. W., 1999). BCl (or maxi Cl⁻) channels are reported to be activated under hypotonic conditions, membrane stretch or by path excision from non-swollen cells (Nilius B. et al., 1997). Also, hypertonicity-induced SCl (or mini Cl⁻) channels with unitary conductances in the range of 2 pS to 10 pS have been reported so far (Christensen O. et al., 1989; Zhang J. J. and Jacob T. J., 1997).

There is an increasing number of reports showing a protein-protein interaction of ENaC and cystic fibrosis transmembrane conductance regulator (CFTR). ENaC is the main pathway for sodium absorption and routinely co-localize with CFTR in the apical membrane of many polarized epithelial cells, including airway, gastrointestinal, and renal cells (Schwiebert E. M. et al., 1999). Reddy M. M. et al., 1999 report that, in freshly isolated normal sweat ducts, ENaC activity is dependent on, and increases with, CFTR activity. As far as electroneutrality is concerned, it is consistent that CFTR and ENaC channels should open together when NaCl (Na^+ and Cl⁻) is absorbed electroconductively. The same group also observed that the primary defect in Cl⁻ permeability in cystic fibrosis is accompanied secondarily by a Na^+ conductance in this tissue that cannot be activated. Some other groups report, that when co-expressed in *Xenopus* oocytes, αβγ-rENaC-induced Na^+ current was inhibited by co-expression of CFTR,

and further inhibited when CFTR was activated with a cAMP-raising mixture (CKT). Conversely, αβγ-rENaC stimulated CFTR-mediated Cl⁻ currents up to ~6-fold (Ji H. L. et al., 2000; Kunzelmann K. 2001).

Altogether, our results and the previous findings suggest a possible interplay between cation and anion conductance under hypertonic stress and during RVI.

4.2.2 α-ENaC and RVI in HepG2 Cells

To investigate the physiology and pathology associated with cell volume regulation, it is important to use an appropriate technique that allows quantitative, high-resolution characterization of cell volume while retaining the cell functionality. Acoustic microscopy has two main advantages when applied to cell biology. Firstly, acoustic microscopy is non invasive and therefore able to provide access to the cells behaviour over prolonged periods of time. Secondly, it can image the local mechanical properties and the geometry of the cell.

The main limitation of the method, however, is the minimal cell thickness required which equals around 3 μm. This causes the data loss in case of working with cells having a relatively small size. Taking into account that HepG2 cell height is about 4 μm it becomes understandable why the measured absolute value of HepG2 cell volume (~ 3 pl) seems to be quite small. As a comparison, rat hepatocytes have been reported to have ~ 7 pl volume measured by SAM (Plettenberg S. et al., 2007). The acoustic microscope recognizes only the part of the cell which corresponds to the cell thickness more then 3 μm threshold. It may also explain the artificially high cell shrinkage values under the hypertonic

conditions. In order to understand this clearly one should consider a Boyle-van't Hoff plot of osmotic cell shrinkage (Figure 4.2) (Wehner F. and Tinel H., 2000).

From the intercept of the regression line with the volume axis (the volume at infinite osmotic pressure) an "osmotically inactive" space (i.e. a non-aqueous volume) of 31.3 ± 5.4 % of the total cell volume can be derived. The same regression line for HepG2 cells obtained by SAM volume measurements looks quite different (Figure 4.3) and would even cross the cell volume axis at a negative value. The non-aqueous volume can not be negative because each cell contains reasonable amount of hydrophobic components. That's why the cell shrinkage up to 60 % at 410 mosmol/l is not possible. Our results may be explained by the loss of the data when the cell undergoes shrinkage. This is very likely considering comparable values of the cell height and 3µm threshold which can be detected by the instrument. Thus, the areas corresponding to the cell height less then 3 µm will be detected as a substrate and the complete volume of the shrunken cell will appear smaller than it is in reality.

Nevertheless, an obvious RVI effect can be measured under this conditions and it doesn't seem to differ too much from the previous studies of RVI in rat and human hepatocytes (Wehner F. and Tinel H., 2000; Wehner F. et al., 2002).
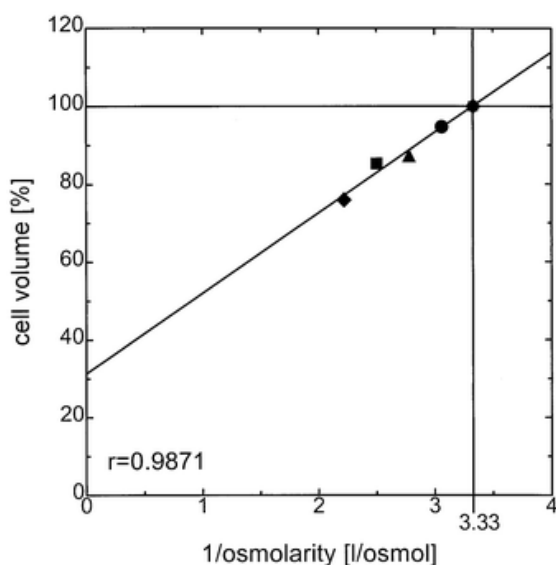
Figure 4.2: Boyle-van't Hoff plot of cell volume measured at 10-min exposure to hypertonicity vs. 1/osmolarity (327, 360, 400, 450 mosmol/l) in the continuous presence of 10-3 mol/l amiloride plus 10-4 mol/l furosemide. The value 3.33 on the axis is equivalent to 300 mosmol/l, at which cell volume is 100 % (control). The solid line shows the linear regression.
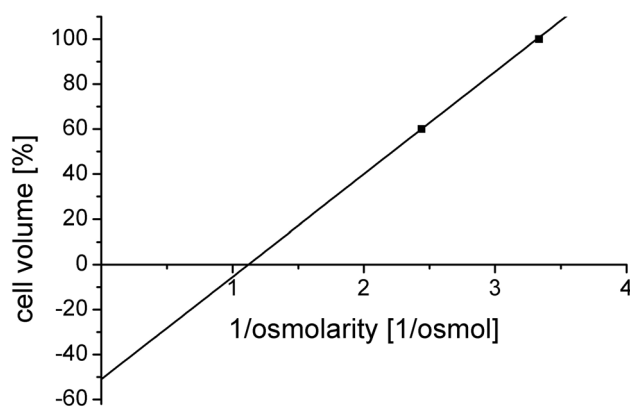
Figure 4.3: Boyle-van't Hoff plot of cell volume measured at 2-3 min exposure to hypertonicity vs. 1/osmolarity (300, 410 mosmol/l). The value 3.33 on the axis is equivalent to 300 mosmol/l, at which cell volume is 100 % (control).

Application of α-ENaC siRNA significantly reduced RVI in HepG2 cells suggesting a sizeable role of α-ENaC in the volume regulation processes of this system and supporting the hypothesis about its molecular correlate with the HICC. The similar observations were made by Plettenberg S. et al. (2007) with regard to rat hepatocytes where siRNA constructs directed against α-, β-, and γ-rENaC significantly reduced RVI as well as HICC currents, altogether rendering a functional correlation between the HICC and the three subunits of the ENaC very likely. It is, however, remaining unclear whether β- and γ-rENaC do indeed contribute to HICC architecture or if they just serve as cofactors for the exocytotic insertion of α-ENaC into the plasma membrane. And this was the main reason why β- and γ-subunits were not tested in the present study.

4.2.3 α-ENaC and HepG2 Cell Proliferation

There are no reports available so far indicating any role of ENaC in the cell proliferation processes. In the present study it was found that transfection of α-ENaC siRNA in HepG2 cells led to the reduction of proliferation to 50% (Vi-CELL counting) and 33% (MTT) with regard to the controls transfected with negative control siRNA. Comparing this data with siRNA transfection efficiency one can conclude that HepG2 cell proliferation is stopped completely under conditions of α-ENaC silencing. Considering α-ENaC to be the part of the HICC along or with some other interacting partners its contribution to proliferation does not seem surprising.

The other mediators of RVI process Na^+/H^+ exchanger and $Na^+/K^+/Cl^-$ cotransporter were shown previously to be essential for the cell cycle progression

in other systems. For example, ethylisopropylamiloride, a selective inhibitor of the Na^+/H^+ exchanger, inhibited the intracellular alkalinization, the migration, and proliferation induced by G- and GM-CSF (Bussolino F. et al., 1989). Amiloride, an Na^+/H^+ exchange inhibitor, reduces PDGF-induced rat hepatic stellate cells (HSC) proliferation, suggesting that the Na^+/H^+ exchanger plays a role in regulating HSC proliferative response (Di Sario A. et al., 1999). $Na^+/K^+/Cl^-$ cotransporter inhibitor bumetanide impaired both, swelling and cell cycle progression (Bussolati O. et al., 1996).

Cell cycle analysis of HepG2 cells demonstrated that transfection reagent and negative control siRNA had no or minor effects on the cells distribution over G1, S, and G2 phases. Silencing of the α-ENaC protein expression by use of specific siRNA (with the same nucleotide composition as in the negative control siRNA) led to the significant decrease in the S phase and non-significant but still obvious increase in G2 phase of the cell cycle. Taking into account that the amount of cells in G1 phase didn't change upon α-ENaC silencing, one can conclude that S phase reduction could be caused by the relative increase in G2 phase. Accumulation of cells in G2 phase with the obvious decrease in their proliferation rate suggests the transit time delay through G2/M phase in HepG2 cells upon α-ENaC silencing.

The observed effect is not devoid of physiological relevance. It is known that intracellular Na^+ shows a continuous change in concentration during the cell cycle. Before a shift in G1/S and G2/M phases the intracellular Na^+ content and cell volume increase (Feltes T. F. et al., 1993). Na^+ concentration is maximal in mitosis and decreases rapidly fourfold as cells enter G1 phase (Mummery C. L. et al., 1982). So remarkable Na^+ perturbations might require the ion channels to be expressed and activated at the particular stages of the cell cycle.

In principle, ion channels may affect proliferation in two different ways: Any cell requires ion channel function to maintain basic homeostatic parameters, such as intracellular Ca^{2+}, pH and cell volume, and to allow uptake of substrates and release of metabolic products. Thus, inhibition of those channels will lower cell proliferation without interfering at a particular step during the cell cycle. On the other hand, ion channel activity, such as the hyperpolarizing activity of K^+ channels, is required at special check points during the cell cycle and therefore will have a precise role in proliferation (Kunzelmann K., 2005). Altogether, these observations suggest the direct contribution of α-ENaC in HepG2 proliferation and cell cycle progression.

4.2.4 Identification of the α-ENaC-Interacting Proteins

Hypertonicity-induced cation channel could be composed of α-ENaC together with some other unknown partners which can perform physical interaction on the plasma membrane. As α-ENaC is identified as a functional component of the HICC, it can be tagged and used as a bait for the following pull-down with its binding partner (the prey). Identification of bait-prey interactions requires that the complex is removed from the affinity support and analyzed by standard protein detection methods. Electrospray ionisation mass spectrometry (ESI-MS) was the first method of choice in our experiments. Nevertheless, following pull-down and analysis of the resulting protein mixture there was nothing identified but α-ENaC and some background proteins. Probably, the problem was the overexpression of bait protein and insufficient amount of the prey proteins in the probe.

First, the different methods for an accurate plasma membrane isolation were chosen in order to reduce intracellular α-ENaC and background proteins. But the result didn't change too much. Then, 1 and 2 dimensional separation of the proteins was employed. Two classical bands (75 and 87 kDa) of α-ENaC and the heavy chain of anti-Flag-antibody (50 kDa) were observed on the 1D gel. But no additional protein bands could be detected in the sample with the DTSSP crosslinking. Once again, the reason could be the α-ENaC overexpression and its possible co-localization with the prey proteins on the gel.

Separation of the proteins in two dimensions did not yield any additional information. Still the prey proteins could not be identified because of overexpression and gel overloading with the bait protein which could just mask the possible interacting partners (the α-ENaC-interacting proteins are supposed to have a molecular mass and isoelectric point close to α-ENaC).

Then it was decided to identify the α-ENaC interacting proteins by Western Blot analysis which could be more sensitive to the low protein amount. But this method is limited by the restricted number of antibodies against the potential prey candidates. Nevertheless, the antibodies against β-, γ-, δ-ENaC subunits, ASIC1, TRPM7, TRPP2, and CFTR were used as the most potent candidates to interact with α-ENaC in the HepG2 plasma membrane.

Amiloride-sensitive ion channels are formed from homo- or heteromeric combinations of subunits from the Epithelial Na^+ Channel (ENaC) / Degenerin superfamily, which also includes the acid sensitive ion channel (ASIC). It was recently demonstrated that ASIC and ENaC subunits are capable of forming cross-clade intermolecular interactions. The subunits of ASIC and ENaC can intermix promiscuously, and the ion channel properties including cation selectivity and

pharmacological inhibition are affected by the subunit composition of the expressed channel (Meltzer R. H. et al., 2007).

TRPM7 has been considered as a candidate for mechanosensation in a variety of cell types. This channel has been demonstrated to be activated by cell stretch and potentiated by hypotonic cell swelling in human epithelial cells (Numata T. et al., 2007). TRPP2 is a widely expressed non-selective cation channel that passes Ca^{2+} (of note, the HICC in human hepatocytes is also Ca^{2+} permeable (Li T. et al., 2006)). And it was shown that the hydro-osmotic pressure has an effect of the channel function in the human syncytiotrophoblasts (Montalbetti N. et al., 2005).

The possible molecular interaction of CFTR with ENaC subunits was already discussed (4.2.1).

Western Blot analysis of HepG2 cell lysates showed that only some of the chosen candidates are expressed in these cells. The classical protein bands were found for γ- and δ-ENaC subunits and for CFTR protein. The bands for TRPM7 protein are quite different from the published observations (220, 160 kDa). Nevertheless, anti-TRPM7 antibody was used in the experiments identifying the α-ENaC interacting proteins.

The pull down experiments with the subsequent SDS-PAGE and Western Blot analysis of the eluted proteins showed that neither of the potential protein candidates is interacting with α-ENaC in the membrane of HepG2 cells. Thus, it remains unclear until now which proteins form the HICC together with α-ENaC in HepG2 cells. Further studies are needed to characterize the overall architecture of the HICC. Screen of the other subfamilies of TRP channels for the interaction with α-ENaC could be the following step in the identification of the HICC protein

partners. Alternatively, α-ENaC interacting proteins could be identified by use of the split-ubiquitin yeast two-hybrid system.

5. Summary

It is becoming increasingly clear that cell volume regulatory mechanisms are critically involved in the regulation of a wide variety of physiological functions including cell proliferation and programmed cell death (apoptosis). In the current study, human hepatoma cell line (HepG2) was chosen as a system to investigate hypertonicity-induced cation channels (HICCs) and their role in hepatocytes proliferation.

Hypertonicity-induced cation conductance is the main mechanism of RVI, which is a restoration process of cell volume after osmotic cell shrinkage. Electrophysiological techniques were used to monitor the activation of HICC current and its pharmacological characteristics in HepG2 cells. In the present study, it was demonstrated that HICC current is inhibited by amiloride, flufenamate and Gd^{3+} in a dose-dependent manner. Next, the concentration dependency of the effects of the same pharmacological compounds on HepG2 cell proliferation was examined. The observed rate of proliferation exhibited a pharmacological profile that was very similar to that of channel inhibition. This was already indicative that the cation channels of RVI may actually function as mediators of proliferation.

With the aid of siRNA technique and whole-cell patch-clamp recordings α-subunit of epithelial sodium channel (ENaC) was identified as a functional

component of the HICC in HepG2 cells. Moreover, it may have a contribution to the basal Na^+ conductance in these cells. Cl^- conductance was shown to be increased under the α-ENaC silencing conditions indicating the interplay of cation and anion conductance under hypertonic stress and during RVI.

By means of Scanning Acoustic Microscopy in combination with siRNA the paramount importance of α-ENaC for RVI process in HepG2 cells could be shown.

Moreover, α-ENaC protein was shown to contribute to HepG2 cell proliferation. Combination of proliferation assays with cell cycle analysis suggests the requirement of α-ENaC for the transition of HepG2 cells from G2 into M phase of the cell cycle.

Finally, to identify the proteins interacting with α-ENaC and to define the overall architecture of the HICC, tagged α-ENaC was overexpressed in HepG2 cells for the pull down of interacting partners. For the identification of precipitated proteins ESI-MS and Western Blot techniques were employed. It was found, that β-, γ-, and δ- subunits of ENaC, as well as TRPM7, TRPP2, ASIC1, and CFTR do very likely not interact with α-ENaC on the HepG2 cell membrane. Thus, the present study does not give a precise answer concerning the complete identity of the HICC. Further studies a needed to fulfill the identification of all the players contributing to the HICC and thus the RVI process as well as cell proliferation in human hepatocytes.

6. Zusammenfassung

Es wird zunehmend deutlich, dass die Mechanismen der zellulären Volumenregulation in kritischem Maße involviert sind an der Regulation einer Reihe von physiologischen Funktionen, wie der Zell Proliferation und dem programmierter Zell Tod (der Apoptose). In der vorliegenden Arbeit wurde die humane Hepatozyten Zelllinie HepG2, als ein System zur Untersuchung der hyperton aktivierten Kationen Kanäle (HICCs) und deren Rolle bei der Proliferation der Hepatozyten ausgewählt.

Die hyperton aktivierte Kationen Leitfähigkeit ist der Hauptmechanismus des RVI, welcher ein Prozess zur Wiederherstellung des Zellvolumens nach osmotischer Zell Schrumpfung ist. Es wurden „*whole-cell patch-clamp*" Ableitungen benutzt, um die Aktivierung von HICC Strömen und die pharmakologischen Charakteristika in HepG2 Zellen zu beobachten. In der vorliegenden Arbeit konnte gezeigt werden, dass die HICC Ströme durch Amiloride, Flufenamat und Gd^{3+} in dosisabhängiger Weise gehemmt werden. Weiter wurde die Konzentrationsabhängigkeit der Effekte der gleichen pharmakologischen Komponenten auf die HepG2 Zellproliferation geprüft. Die beobachtete Proliferationsrate zeigte ein pharmakologisches Profil, welches dem der Kanalinhibierung sehr ähnlich war. Dies wies bereits darauf hin, dass die Kationen Kanäle des RVI als Mediatoren der Proliferation fungieren.

Mit den Hilfsmitteln der siRNA Technik und „*whole-cell patch-clamp*" Ableitungen wurde die α Untereinheit des epithelialen Natrium Kanals (ENaC) als funktionelle Komponente des HICC in HepG2 Zellen identifiziert. Ferner könnte eine Beteiligung von α-ENaC an der basalen Na^+ Leitfähigkeit in diesen Zellen vorliegen. Für die Cl^- Leitfähigkeit konnte eine Zunahme unter α-ENaC geminderten Bedingungen gezeigt werden, was für ein Zusammenspiel von Kationen- und Anionen- Leitfähigkeiten unter hypertonem Stress und während des RVI spricht.

Durch die Methode der „*Scanning Acoustic Microscopy*" in Kombination mit siRNA konnte die überragende Bedeutung der α-ENaC Untereinheit für den RVI Prozess in HepG2 Zellen gezeigt werden.

Darüber hinaus konnte eine Beteiligung des α ENaC Proteins an der HepG2 Zellproliferation gezeigt werden. Eine Kombination aus Prolifertions- Analysen und Zellzyklus- Analysen legt nahe, dass HepG2 Zellen die α-ENaC Untereinheit benötigen, um von der G2 Phase in die M Phase des Zellzyklus fortschreiten zu können.

Schließlich wurden, um Interaktionspartner von α ENaC und den allgemeinen Aufbau des HICC Kanals zu identifizieren, markierte α-ENaC Untereinheiten überexprimiert, um Interaktionspartner zu isolieren. Für die Identifizierung der präzipitierten Proteine kamen ESI-MS und die Methode des „*Western Blot*" zum Einsatz. Es wurde heraus gefunden, dass sowohl die β-, γ-, und δ-Untereinheiten des ENaC, als auch TRPM7, TRPP2, ASIC1 und CFTR höchst wahrscheinlich nicht mit α-ENaC an der HepG2 Zellmembran interagieren.

Demnach, kann die vorliegende Arbeit keine präzise Antwort auf die Frage der kompletten Identität des HICC geben. Weitere Studien müssen erbracht werden, um die Identität aller beteiligten Akteure des HICC und somit des RVI und als auch der Zellproliferation in humanen Hepatozyten zu klären.

7. Abbreviations

AP1	Activator protein 1
ASIC	Acid-sensing Ion Channel
ATP	Adenosine triphosphate
AVD	Apoptotic volume decrease
BSA	Bovine serum albumin
CFTR	Cystic fibrosis transmembrane conductance regulator
CHAPS	3-[(3-Cholamidopropyl)dimethylammonio]-1-propanesulfonate
DAPI	4'-6-Diamidine-2-phenylindol
dNTP	Dinucleotidtriphosphate
DTSSP	3,3′-dithiobis (sulfosuccinimidylpropionate)
DTT	dithiothreitol
ECL	Enhanced chemiluminescence
EDTA	Ethylenediaminetetraacetic acid
EGTA	Ethylene glycol tetraacetic acid
ENaC	Epithelial sodium channel
Erk	Extracellular-signal-regulated kinase
ESI-MS	Electrospray ionisation mass spectrometry
FACS	Fluorescence-Activated Cell Sorter
FCS	fetal calf serum
Gd^{3+}	gadolinium III
GTP	Guanin nucleotide triphosphate
HEPES	4-(2-hydroxyethyl)-1-piperazineethanesulfonic acid
HepG2	Human hepatoma cell line
HICC	Hypertonicity-induced cation channel

HRP	Horseradish peroxidase
IEF	Isoelectric focusing
LB medium	Luria-Bertani medium
MALDI-MS	matrix assisted laser desorption/ionization - mass spectrometry
MAP kinase	Mitogen-activated protein kinase
MES	2-(N-morpholino)ethanesulfonic acid
MTT	3-[4,5-dimethylthiazol-2-yl]-2,5-diphenyl tetrazolium bromide
NF-κB	Nuclear factor kappa B
NHE	Na^+/H^+ exchanger
NKCC	Na^+-K^+-$2Cl^-$ cotransporter
ORCC	outwardly rectifying Cl^- channel
PAGE	Polyacrylamid gelelectrophoresis
PBS	Phosphate buffered saline
PCR	Polymerase Chain Reaction
PFA	Paraformaldehyde
PI 3	Phosphoinositide 3
PVDF	Polyvinylidenfluorid
RVD	Regulatory volume decrease
RVI	Regulatory volume increase
SAM	Scanning acoustic microscopy
SDS	Sodium dodecyl sulfate
SEM	Standard error of the mean
TBST	Tris buffered saline
TEA-C	tetraethylammonium chloride
TGF	Tumor necrosis factor
TRP	Transient receptor potential
Vm	Membrane voltage

8. References

Achard,J.M., Bubien,J.K., Benos,D.J., and Warnock,D.G. Stretch modulated amiloride sensitivity and cation selectivity of sodium channels in human B lymphocytes. *Am. J. Physiol.* 1996; 270: C224 – C234.

Anbari,K., Schultz,R.M. Effect of sodium and betaine in culture media on development and relative rates of protein synthesis in preimplantation mouse embryos in vitro. *Mol. Reprod. Dev.* 1993; 35: 24 – 28.

Askwith,C.C., Benson,C.J., Welsh,M.J., Snyder,P.M. DEG/ENaC ion channels involved in sensory transduction are modulated by cold temperature. *Proc. Natl. Acad. Sci.* USA 2001; 98: 6459 – 6463.

Awada,M.S., Ismailov,I.I., Berdiev,B.K., and Benos,D.J. A cloned renal epithelial Na^+ channel protein displays stretch activation in planar lipid bilayers. *Am. J. Physiol.* 1995; 268 : C1450 – C1459.

Baldetorp,B., Stal,O., Ahrens,O., Cornelisse,C., Corver,W., Falkmer,U., Ferno,M. Different calculation methods for flow cytometric S-phase fraction: prognostic implication in breast cancer. *Cytometry* 1998; 33: 385 – 393.

Beech,D.J., Muraki,K., Flemming,R. Non-selective cation channels of smooth muscle and the mammalian homologues of Drosophila TRP. *J. Physiol.* 2004; 559: 685 – 706.

Bianchini,L., Grinstein,S. Regulation of volume-modulating ion transport systems by growth promoters. *Adv. Comp. Env. Physiol.* 1993; 14: 249–270.

Böhmer,C., Wagner,C.A., Beck,S., Moschen,I., Melzig,J., Werner,A., Lin,J.T., Lang,F., Wehner,F. The Shrinkage-activated Na^+ Conductance of Rat Hepatocytes and its Possible Correlation to rENaC. *Cell. Physiol. Biochem.* 2000; 10: 187 – 194.

Böhmer,C., Wehner,F. The epithelial Na^+ channel (ENaC) is related to the hypertonicity-induced Na^+ conductance in rat hepatocytes. *FEBS Lett.* 2001; 494: 125 – 128.

Bortner,C.D., Cidlowski,J.A. Absence of volume regulatory mechanisms contributes to the rapid activation of apoptosis in thymocytes. *Am. J. Physiol.* 1996; 40: C 950-C 961.

Bradford,M.M. A rapid and sensitive method for the quantitation of microgram quantities of protein utilizing the principle of protein-dye binding 4. *Anal. Biochem.* 1976; 72: 248-254.

Burger,C., Wick,M., Brusselbach,S., Muller,R. Differential induction of „metabolic genes" after mitogen stimulation and during normal cell cycle progression. *J. Cell Sci.* 1994; 107: 241 – 252.

Bussolati,O., Uggeri,J., Belletti,S., Dallasta,V., Gazzola,G.C. The stimulation of $Na^+/K^+/Cl^-$ cotransport and of system AS for neutral amino acids transport is a mechanism for cell volume increase during the cell cycle. *FASEB. J.* 1996; 10: 920 – 926.

Bussolino,F., Wang,J.M., Turrini,F., Alessi,D., Ghigo,D., Costamagna,C., Pescarmona,G., Mantovani,A., Bosia,A. Stimulation of the Na^+/H^+ exchanger in human endothelial cells activated by granulocyte- and granulocyte-macrophage-colony-stimulating factor. Evidence for a role in proliferation and migration. *J. Biol. Chem.* 1989; 264: 18284 – 18287.

Caldwell,R.A., Clemo,H.F., Baumgarten,C.M. Using gadolinium to identify stretch-activated channels: technical considerations. *Am. Physiol. Soc.* 1998; C619 - C621.

Canessa,C.M., Schild,L., Buell,G., Thorens,B., Gautschl,I., Horisberger,J.D., Rossier,B.C. *Nature* 1994; 367: 463 – 467.

Carattino,M.D, Sheng,S., Kleyman,T.R. Epithelial Na^+ channels are activated by laminar shear stress. *J. Biol. Chem.* 2004; 279: 4120 – 4126.

Chan,H.C and Nelson,D.J. Chloride-dependent cation conductance activated during cellular shrinkage. *Science* 1992; 257: 669 – 671.

Christensen,O., Simon,M., Randlev,T. Anion channels in a leaky epithelium. A patch-clamp study of choroid plexus. *Pflügers Arch.* 1989; 415: 37 – 46.

Ciura,S. and Bourque,C.W. Transient receptor potential vanilloid 1 is required for intrinsic osmoreception in organum vasculosum lamina terminalis neurons and for normal thirst responses to systemic hyperosmolality. *J. Neurosci.* 2006; 26: 9069 – 9075.

d'Anglemont-de-Tassigny,A., Ghaleh,B., Souktani,R., Henry,P., Berdeaux,A. Hypoosmotic stress inhibits doxorubicin-induced apoptosis via a protein kinase A-dependent mechanism in cardiomyocytes. *Clin. Exp. Pharmacol. Physiol.* 2004; 31: 438 – 443.

Di Sario,A., Bendia,E., Baroni,G.S., Ridolfi,F., Bolognini,L., Filiciangeli,G., Jezequel,A.M., Orlandi,F., Benedetti,A. Intracellular pathways mediating Na^+/H^+ exchanger activation by platelet-derived growth factor in rat hepatic stellate cells. *Gastroenterology* 1999; 116: 1155 – 1166.

Dijkink,L., Hartog,A., van Os,C.H., Bindels,R.J.M. The epithelial sodium channel (ENaC) is intracellularly located as a tetramer. *Pflüg.Arch. Eur. J. Physiol.* 2002; 444: 549 – 555.

Dingley,A.J., Veale,M.F., King,N.J., King,G.F. Two-dimensional H NMR studies of membrane changes during the activation of primary T lymphocytes. *Immunomethods* 1994; 4: 127 – 138.

Feltes,T.F., Seidel,C.L., Dennison,D.K., Amick,S., Allen,J.C. Relationship between functional Na$^+$ pumps and mitogenesis in cultures coronary artery smooth muscle cells. *Am. J. Physiol. Cell Physiol.* 1993; 264: C169 – C178.

Feltes,T.F., Seidel,C.L., Dennison,D.K., Amick,S., Allen,J.C. Relationship between functional Na$^+$ pumps and mitogenesis in cultures coronary artery smooth muscle cells. *Am. J. Physiol.* 1993; 264: C169 – C178.

Freeman,T.L., Ngo,H.Q., Mailliard,M.E. Inhibition of system A amino acid transport and hepatocytes proliferation following partial hepatectomy in the rat. *Hepatology* 1999; 30: 437 – 444.

Gamper,N., Huber,S.M., Badawi,K., Lang,F. Cell volume-sensitive sodium channels upregulated by glucocorticoids in U937 macrophages. *Pflügers Arch.* 2000; 441: 281 – 286.

Garty,H., Palmer,L.G. Epithelial sodium channels: function, structure, and regulation. *Physiol. Rev.* 1997; 77: 359 – 396.

Gründer,S., Thiemann,A., Pusch,M., Jentsch,T.J. Regions involved in the opening of ClC-2 chloride channel by voltage and cell volume. *Nature* 1992; 360: 759 – 762.

Hanwell,D., Ishikawa,T., Saleki,R., Rotin,D. Trafficking and cell surface stability of the epithelial Na$^+$ channel expressed in epithelial MDCK cells. *J. Biol. Chem.* 2002; 277: 9772 – 9779.

Häussinger,D., Schliess,F., Warskulat,U. and vom Dahl,S. Liver cell hydration. *Cell Biol. Toxicol.* 1997; 13: 275-87.

Higgins,C.F., Cairney,J., Stirling,D.A., Sutherland,L., Booth,I.R. Osmotic regulation of gene expression: Ionic strength as an intracellular signal? *Trends. Biochem. Sci.* 1987; 12: 339 – 344.

Hoffmann,E.K., Mills,J.W., Membrane events involved in volume regulation. *Curr. Top. Membr.* 1999; 48: 123 – 196.

Huber,S.M., Gamper,N., Lang,F. Chloride conductance and volume-regulatory nonselective cation conductance in human red blood ghosts. *Pflügers Arch.* 2001, 441: 551 – 558.

Hume,J.R., Duan,D., Collier,M.L., Yamazaki, J., Horowitz,B. Anion transport in heart. *Physiol. Rev.* 2000; 80: 31 – 81.

Iwamoto,L.M., Fujiwara,N., Nakamura,K.T., Wada,R.K. $Na^+/K^+/2Cl^-$ cotransporter inhibition impairs human lung cellular proliferation. *Am. J. Physiol.* 2004; 287: L510-L514.

Jackson,P.S., Morrison,R., Strange,K. The volume-sensitive organic osmolytes-anion channel VSOAC is regulated by nonhydrolytic ATP binding. *Am. J. Physiol.* 1994; 267: C1203 – C1209.

Jain,L., Chen,X.J., Ramosevac,S., Brown,L.A., Eaton,D.C. Expression of highly selective sodium channels in alveolar type II cells is determined by culture conditions. *Am J. Physiol. Lung Cell Mol. Physiol.* 2001; 280: L646 – L658.

Ji,H.L., Chalfant,M.L., Jovov,B., Lockhart,J.P., Parker,S.B., Fuller,C.M., Stanton,B.A., Benos,D.J. The cytosolic termini of the β- and γ-ENaC subunits are involved in the functional

interactions between cystic fibrosis transmembrane conductance regulator and epithelial sodium channel. *J. Biol. Chem.* 2000; 275: 27947 – 27956.

Ji,H.L., Fuller,C.M., and Benos,D.J. Osmotic pressure regulates αβγ-rENaC expressed in Xenopus oocytes. *Am. J. Physiol.* 1998; 275: C1182 – C1190.

Ji,H.L., Fuller,C.M., Benos,D.J. Osmotic pressure regulates αβγ-rENaC expressed in Xenopus oocytes. *Am. J. Physiol.* 1998; 275: C1182 – C1190.

Kellenberger,S., Gautschi,I., Schild,L. A single point mutation in the pore region of the epithelial Na^+ channel changes ion selectivity by modifying molecular sieving. *Proc. Natl. Acad. Sci.* USA 1999; 96: 4170 – 4175.

Kellenberger,S., Hoffmann-Pochon,N., Gautschi,I., Schneeberger,E., Schild, L. On the molecular basis of ion permeation in the epithelial Na^+ channel. *J. Gen Physiol.* 1999; 114: 13 – 30.

Kellenberger,S. Schild,L. Epithelial sodium channel/degenerin family of ion channels: a variety of functions for a shared structure. *Physiol. Rev.* 2002; 82: 735 – 767.

Kizer,N., Guo,X.L., Hruska,K. Reconstitution of stretch-activated cation channels by expression of the α-subunit of the epithelial sodium channel cloned from osteoblasts. *Proc. Natl. Acad. Sci.* 1997; 94: 1013 – 1018.

Kleyman,T.R., Cragoe,E.J. Amiloride and its analogs as tools in the study of ion transport. *J. Membr. Biol.* 1988; 105: 1 – 21.

Kleyman,T.R., Zuckerman,J.B., Middleton,P., McNulty,K.A., Hu,B., Su,X., An,B., Eaton,D.C., Smith,P.R. Cell surface expression and turnover of the α-subunit of the epithelial sodium channel. *Am. J. Physiol. Renal. Physiol.* 2001; 281: F213 – F221.

Koch,J.P., Korbmacher,C. Osmotic shrinkage activates nonselective cation (NSC) channels in various cell types. *J. Membr. Biol.* 1999; 168: 131 – 139.

Koch,K.S., Leffert,H.L. Increased sodium influx is necessary to initiate rat hepatocyte proliferation. *Cell* 1979; 18: 153 – 163, 1979.

Kosari,F., Shen,S., Li,J., Mak,D.D., Foskett,J.K. Subunit stoichiometry of the epithelial sodium channel. *J. Biol. Chem.* 1998; 273: 13469 – 13474.

Kubo,M. and Okada,Y. Volume-regulatory Cl$^-$ channel currents in cultured human epithelial cells. *J. Phys.* 1992; 456: 351–371.

Kunzelmann,K. CFTR: interacting with everything? *News. Physiol. Sci.* 2001; 16: 167 – 170.

Kunzelmann,K. Ion channels and cancer. *Membr. Biol.* 2005; 205: 159 – 173.

Lang,F. Cell volume regulation. *Contrib. Nephrol. Basel*. Karger. 1998; 123: 1 - 7.

Lang,F., Madlung,J., Bock,J., Lukewille,U., Kaltenbach,S., Lang,K.S., Belka,C., Wagner,C.A., Lang,H.J., Gulbins,E., Lepple-Wienhues,A. Inhibition of Jurkat-Tlymphocyte Na$^+$/H$^+$-exchanger by CD95(Fas/Apo-1)-receptor stimulation. *Pflügers Arch.* 2000; 440: 902-907.

Lang,F., Ritter,M., Wöll,E., Weiss,H., Häussinger,D., Hoflacher,J., Maly,K., Grunicke,H. Altered cell volume regulation in ras oncogene expressing NIH fibroblasts. *Pflügers Arch.* 1992; 420: 424 – 427.

Lawitts,J.A., Biggers,J.D. Joint effects of sodium chloride, glutamine, and glucose in mouse preimplantation embryo culture media. *Mol. Reprod. Dev.* 1992; 31: 189 – 194.

Lawonn,P., Hoffmann,E.K., Hougaard,C., Wehner,F. A cell shrinkage-induced non-selective cation conductance with a novel pharmacology in Ehrlich-Lettre-ascites tumour cells. *FEBS Lett.* 2003; 539: 115 – 119.

Lepple-Wienhues,A., Szabo,I., Laun,T., Kaba,N.K., Gulbins,E., Lang,F. The tyrosine kinase p56lck mediates activation of swelling-induced chloride channels in lymphocytes. *J. Cell Biol.* 1998; 141: 281-286.

Li,T., ter Feld,F., Nürnbeger,H.R., Wehner,F. A novel hypertonicity-induced cation channel in primary culture of human hepatocytes. *FEBS Lett.* 2005; 579: 2087 – 2091.

Liedtke,W., Choe,Y., Marti-Renom,M.A., Bell,A.M., Denis,C.S., Sali,A., Hudspeth,A.J., Friedman,J.M., Heller,S. Vanilloid receptor-related osmotically activated channel (VR-OAC), a candidate vertebrate osmoreceptor. *Cell* 2000; 103: 525 – 535.

Lindemann,B. Taste reception. *Physiol. Rev.* 1996; 176: 719 – 766.

Lu,G., Henderson,D., Liu,L., Reinhart,P.H., Simon,S.A. TRPV1b: A functional human vanilloid receptor splice variant. *Mol. Pharmacol.* 2005; 67: 1119 – 1127.

Ma,P.H., Al Khalili,O., Ramosevac,S., Saxena,S., Liang,Y.Y., Warnock,D.G., Eaton,D.C. Steroids and exogenous gamma-ENaC subunit modulate cation channels formed by alpha-ENaC in human B lymphocytes. *J. Biol. Chem.* 2004; 279: 33206 – 33212.

Machida,K., Nonoguchi,H., Wakamatsu,S., Inoue,H. , Yosifovska,T., Inoue,T., Tomita,K. Acute regulation of the epithelial sodium channel gene by vasopressin and hyperosmolality. *Hypertens. Res.* 2003; 26: 629 – 634.

Martinak,B. Mechanosensitive ion channels: molecules of mechanotransduction. *J. Cell Sci.* 2004; 117: 2449 – 2460.

Matalon,S., Lazrak,A., Jain,L., Eaton,D.C. Invites review: biophysical properties of sodium channels in lung alveolar epithelial cells. *J. Appl. Physiol.* 2002; 93: 1852 – 1859.

McNicholas,C.M. and Canessa,C.M. Diversity of Channels generated by different combinations of epithelial sodium channel subunits. *J. Gen. Physiol.* 1997; 109: 681 – 692.

Meltzer,R.H., Kapoor,N., Qadri,Y.J., Anderson,S.J., Fuller,C.M., Benos,D.J. Heteromeric assembly of acid sensitive ion channel and epithelial sodium channel subunits. *J. Biol. Chem.* 2007; 282: 25548 – 25559.

Michalke,M., Cariers,A., Schliess,F., Häussinger,D. Hypoosmolarity influences the activity of transcription factor NF kB in rat H4IIE hepatoma cells. *FEBS Lett.* 2000; 465: 64-68.

Montalbetti,N., Li,Q., Gonzalez-Perrett,S., Semprine,J., Chen,X.Z., Cantiello,H.F. Effect of hydro-osmotic pressure on polycystin-2 channel function in the human syncytiotrophoblast. *Pflüg. Arch. Eur. J. Physiol.* 2005; 451: 294 – 303.

Mullis,K., Faloona,F., Scharf,S., Saiki,R., Horn,G., and Erlich,H. Specific enzymatic amplification of DNA in vitro: the polymerase chain reaction. *Cold Spring Harb. Symp. Quant. Biol.* 1986; 51:263 – 273.

Mummery,C.L., BoonstraJ., van der Saag,P.T., de Laat,S.W. Modulations of Na^+ transport during the cell cycle of neuroblastoma cells. *J. Cell Physiol.* 1982; 112: 27 – 34.

Muraki,K., Iwata,Y., Katanosaka,Y., Ito,T., Ohya,S., Shigekawa,M., Imaizumi,Y. TRPV2 is a component of osmotically sensitive cation channels in murine aortic myocytes. *Circ. Res.* 2003; 93: 829 – 838.

Naeini,R.S., Witty,M.F., Seguela,P., and Bourque,C.W. An N-terminal variant of Trpv1 channel is required for osmosensory transduction. *Nat. Neurosci.* 2005; 9: 93 – 98.

Needham,D. Possible role of cell cycle-dependent morphology, geometry, and mechanical properties in tumor cell metastasis. *Cell. Biophys.* 1991; 18: 99 – 121.

Nelson,D.J., Tien,X.Y., Xie,W.W., Brasitus,T.A., Kaetzel,M.A., Dedman,J.R. Shrinkage activates a non-selective cation conductance: involvement of a Walker-motif protein and PKC. *Am. J. Physiol.* 1996; 270: C179 – C 191.

Nilius,B., Droogmans,G. Ion channels and their functional role in vascular endothelium. *Physiol. Rev.* 2001; 81: 1415 – 1459.

Nilius,B., Eggermont,J., Voets,T., Buyse,G., Manolopoulos,V., Droogmans,G. Properties of volume-regulated anion channels in mammalian cells. *Prog. Biophys. Mol. Biol.* 1997; 68: 69 – 119.

Nilius,B., Prenen,J., Wissenbach,U., Bodding,M., Droogmans,G. Differential activation of the volume-sensitive cation channel TRP12 (OTRPC4) and volume-ragulated anion currents in HEK-293 cells. *Pflüg. Arch. Eur. J. Physiol.* 2001; 443: 227 – 233.

Numata,T., Shimizu,T., Okada,Y. TRPM7 is a stretch- and swelling-activated cation channel involved in volume regulation in human epithelial cells. *Am. J. Physiol. Cell Physiol.* 2007; 292: C460 – C467.

Okada,Y. Volume expantion-sensing outward-rectifier Cl⁻ channel: fresh start to the molecular identity and volume sensor. *Am. J. Physiol.* 1997; 273: C755 – C789.

Olsen,H., ter Veld,F., Herbrand,U., Ahmadian,M.R., Kinne,R.K.H. and Wehner,F. Differential regulation of cell volume and shape in confluent rat hepatocytes under hypertonic stress. *Cell Physiol. Biochem.* 2007; 19: 259-268.

Panet R., Atlan H. Overexpression of the $Na^+/K^+/2Cl^-$ cotransporter gene induces cell proliferation and phenotypic transformation in mouse fibroblasts. *J. Cell Physiol.* 182: 109-118, 2000.

Pedersen,S.F. and Nilius,B. Transient receptor potential channels in mechanosensing and cell volume regulation. *Meth. Enzym.* 2007; 428: 183 – 207.

Petronini,P.G., De Angelis,E.M., Borghetti,P., Wheeler,K.P. Modulation of betaine of cellular responses to osmotic stress. *Biochem. J.* 1992; 282: 69 – 73.

Plettenberg,S., Weiss,E.C., Lemor,R., Wehner,F. Subunits α, β and γ of the epithelial Na^+ channel (ENaC) are functionally related to the hypertonicity-induced cation channel (HICC) in rat hepatocytes. *Pflug. Arch. Eur. J. Physiol.* 2007, in press.

Poronnik,P., Ward,M.C., Cook,D.I. Intracellular Ca2+ release by Flufenamic acid and other blockers of the non-selective cation channel. *FEBS Lett.* 1992; 296: 245 – 248.

Poulmichl,M., Li,Y., Wickman,K., Ackerman,M., Peralta,E., Clapham,D. New mammalian chloride channel identified by expression cloning. *Nature* 1992; 356: 238 – 241.

Reddy,M.M., Light,M.J., Quinton,P.M. Activation of the epithelial Na^+ channel (ENaC) requires CFTR Cl- channel function. *Nature* 1999; 402: 301 – 304.

Ritter,M., Wöll,E. Modification of cellular ion transport by the Ha-Ras oncogene: steps towards malignant transformation. *Cell. Physiol. Biochem.* 1996; 6: 245 – 270.

Rotin,D., Kanelis,V., and Schild,L. Trafficking and cell surface stability of ENaC. *Am. J. Physiol. Renal. Physiol.* 2001; 281: F391 – F399.

Rozengurt,E. Early sinals in the mitogenic response. *Science* 1986; 234: 161 – 166.

Sanger,F., Nicklen,S., and Coulson,A.R. DNA sequencing with chainterminating inhibitors. *Proc. Natl. Acad. Sci.* 1977; 74: 5463-5467.

Satlin,L.M., Sheng,S., Woda,C.B., Kleyman,T.R. Epithelial Na^+ channels are regulated by flow. *Am. J. Physiol. Renal. Physiol.* 2001; 280: F1010 – F1018.

Schild,L. The epithelial sodium channels: from molecule to disease. *Rev. Physiol. Biochem. Pharmacol.* 2004; 151: 93-107.

Schild,L., Schneeberger,E., Gautschi,I., Firsov,D. Identification of amino acid residues in the α, β, and γ subunits of the epithelial sodium channel (ENaC) involved in amiloride block and ion permeation. *J. Gen. Physiol.* 1997; 109: 15 – 26.

Schliess,F., Häussinger,D. The cellular hydration state: role in apoptosis and proliferation. *Signal Transduction* 2005; 6: 297 – 302.

Schwiebert,E.M., Benos,D.J., Egan,M.E., Stutts,M.J., Guggino,W.B. CFTR is a conductance regulator as well as a chloride channel. *Physiol. Rev.* 1999; 79: S145 – S166.

Sheng,S., Li,J., McNulty,K.A., Avery,D., Kleyman,T.R. Characterization of the selectivity filter of the epithelial sodium channel. *J. Biol. Chem.* 2000; 275: 8572 – 8581.

Shimizu,T., Wehner,F., Okada,Y. Inhibition of hypertonicity-induced cation channels sensitizes HeLa cells to shrinkage-induced apoptosis. *Cell. Physiol. Biochem.* 2006; 18: 295 – 302.

Shimkets,R.A., Lifton,R.P., and Canessa,C.M. The activity of the epithelial sodium channel is regulated by clathrin-mediated endocytosis. *J. Biol. Chem.* 1997; 272: 25537 – 25541.

Snyder,P.M., Cheng,C., Prince,L.S., Rogers,J.C., and Welsh,M.J. Electrophysiological and biochemical evidence that DEG/ENaC cation channels are composed of nine subunits. *J. Biol. Chem.* 1998: 273: 681 – 684.

Spassova,M.A., Hewavitharana,T., Xu,W., Soboloff,J., Gill,D.L. A common mechanism underlies stretch activation and receptor activation of TRPC6 channels. *Proc. Natl. Acad. Sci.* 2006; 103: 16586 – 16591.

Stal,O., Baldetorp,B. S-phase fraction assessed by a variant of the rectangular model adapted to the flow-cytometric DNA histogram profile. *Cytometry* 1998; 33: 487 – 491.

Staub,O., Gautschi,I., Ishikawa,T., Breitschopf,K., Ciechanover,A., Schild,L., and Rotin,D. Regulation of stability and function of the epithelial Na^+ channel (ENaC) by ubiquitination. *Embo. J.* 1997; 16: 6325 – 6336.

Strotmann,R., Harteneck,C., Nunnenmacher,K., Schultz,G., Plant,T.D. OTRPC4, a nonselective cation channel that confers sensitivity to extracellular osmolarity. *Nat. Cell Biol.* 2000; 2: 695 – 702.

Takahashi,A., Yamaguchi,H., Miyamoto,H. Change in K^+ current of HeLa cells with progression of the cell cycle studied by path-clamp technique. *Am. J. Physiol.* 1993; 265: C328 – C336.

Venkatachalam,K. and Montell,C. TRP channels. *Annu. Rev. Biochem.* 2007; 76: 387 – 417.

Volk,T., Frömter,E., Korbmacher,C. Hypertonicity avtivates nonselective cation channels in mouse cortical collecting duct cells. *Proc. Natl. Acad. Sci*. 1995; 92: 8478 – 8482.

Wehner,F. Cell volume-Regulated Cation Channels. Contrib. *Nephrol. Basel. Karger*. 2006; 152: 25 – 53.

Wehner,F., Bondarava,M., ter Feld,F., Endl,E., Nürnberger,H.R., Li,T. Hypertonicity-induced cation channels. *Acta Physiol. Scand*. 2006; 187: 21 – 25.

Wehner,F., Lawonn,P., Tinnel,H. Ionic mechanisms of regulatory volume increase (RVI) in the human hepatoma cell-line HepG2. *Pflüg. Arch. Eur. J. Physiol.* 2002; 443: 779-790.

Wehner,F., Olsen,H., Tinel,H., Kinne-Saffran,E., Kinne,R.K.H. Cell volume regulation: osmolytes, osmolyte transport, and signal transduction. *Rev. Physiol. Biochem. Pharmacol*. 2003; 148: 1-80.

Wehner,F., Sauer,H., and Kinne,R.K.H. Hypertonic stress increases the Na$^+$ conductance of rat hepatocytes in primary culture. *J. Gen. Physiol*. 1995; 105: 507 – 535.

Wehner,F., Shimitzu,T., Sabirov,R., Okada,Y. Hypertonic activation of a non-selective cation conductance in HeLa cells and its contribution to cell volume regulation. *FEBS Lett*. 2003; 551: 20 – 24.

Weiss,E.C., Wehner,F., Lemor,R.M. Measuring cell volume regulation with time resolved acoustic microscopy. *Acoustical Imaging* 2007; 73-80.

Weisz,O.A., Wang,J.M., Edinger,R.S., and Johnson,J.P. Non-coordinate regulation of endogenous epithelial sodium channel (ENaC) subunit expression at the apical membrane of A6 cells in response to various transporting conditions. *J. Biol. Chem*. 2000; 275: 39886 – 39893.

Wersto,R.P., Chrest,F.J., Leary,J.F., Morris,C., Stetler-Stevenson,M.A., Gabrielson,E. Doublet discrimination in DNA cell-cycle analysis. *Cytometry* 2001; 46: 296 – 306.

Wu,K.L., Khan,S., Lakhe-Reddy,S., Wang,L., Jarad,G., Miller,R.T., Konieczkowski,M., Brown,A.M., Sedor,J.R., Schelling,J.R. Renal tubular epithelial cell apoptosis is associated with caspase cleavage of the NHE1 Na^+/H^+ exchanger. *Am. J. Physiol*. 2003; 284: F829-F839.

Yamamoto,T., Mundy,C.A., Wilson,C.B., Blantz,R.C. Effect of mesanglial cell lysis and proliferation on glomerular hemodynaics in the rat. *Kidney Int*. 1991; 40: 705 – 713.

Yancey,P.H., Burg,M.B., Bagnasco,S.M. Effect of NaCl, glucose and aldose reductase inhibitors on cloning efficiency of renal medullary cells. *Am. J. Physiol*. 1990; 258: C156 – C163.

Yang,X.C., Sachs,F. Block of stretch-activated ion channels in Xenopus oocytes by gadolinium and calcium ions. *Science* 1989; 243: 1068 – 1071.

Zhang,J.J., Jacob,T.J. Three different Cl^- channels in the bovine ciliary epithelium activated by hypotonic stress. *J. Physiol*. 1997; 499: 379 – 389.

Danksagung

Finishing this work I would like to thank a lot of people who was quite generous in sharing their time and experience with me during these three years.

First of all, I wish to thank Prof. Dr. Frank Wehner for committing to me such an excellent theme and the able supervision. I also thank him for providing me the perfect working conditions and for introducing me to the field of cell biology and biophysics.

I wish to thank Prof. Dr. Dr. Dr. med. habil. Hanns Hatt for the continuous interest and guidance of my work.

Special thanks to Prof. Dr. Dr. h. c. Rolf K. H. Kinne for his invaluable help and nice suggestions in the early stage of the project.

I am very grateful to Prof. Dr. Philippe Bastiaens for his interest, nice discussions, and financial support.

I thank a lot Dr. Tongju Li for introducing me to the patch-clamp, nice discussions and very helpful suggestions during the whole period of my PhD.

Sandra, thank you very much for numerous discussions, wonderful company, and excellent writing the Zusammenfassung. Nina, you are a nice colleague, it was pleasant to work together.

I am grateful to Dr. Takahiro Shimizu and Dr. Elmar Endl for the technical help and discussions.

A lot of thanks to Gabi Beetz, Hendrike Schütz, Jutta Luig, Kirsten Michel for shearing some methodological secrets, technical support and the lovely

atmosphere in the lab. I also thank Petra Glitz and Christiane Pfaff for their help and advice in cell culture.

I thank all the current and former members of the department for their help, discussions and good time.

I thank Prof. Dr. Martin Engelhart and Dr. Jutta Roetter for their support and the International Max Planck Research School in Chemical Biology for financial assistance.

Finally, but immensely, I thank my husband Alexey for being always there for me and my parents for their perpetual love and support.

Lebenslauf

Persönliche Daten

Name:	Maryna Bondarava
Geburtsdatum:	23.11.1981
Geburtsort:	Minsk, Weissrussland
Nationalität:	weissrussisch
Adresse:	Lenteninsel 17
	44143 Dortmund
	Deutschland

Ausbildung

1997 – 1999	Abitur am F. Scorina-Gymnasium, Minsk
1999 – 2004	International Sakharov Environmental University (ISEU), Minsk
06/2003 – 09/2003	Sommer Studentin. Abt. Epithelphysiologie am Max-Planck-Institut für Moleculare Physiologie, Dortmund
2004 – 2007	Promotionsarbeit in der Abteilung für Systemische Zellbiologie am Max-Planck-Institut für Moleculare Physiologie, Dortmund
Februar 2008	Promotion an der Fakultät füt Biologie der Ruhr Universität Bochum

Publikation

Wehner,F., Bondarava,M., ter Veld,F., Endl,E., Nürnberger,H.R., Li,T. Hypertonicity-induced cation channels. Acta Physiol. 2006; 187: 21 – 25.

Abstracts

Scharlau,D., Bondarava,M., Kinne,R.K., Kipp,H. Dynamics of GFP-SGLT1 in COS 7 Cells. *Eur. J. Physiol*. 2004; 447: Suppl. 1.

Scharlau,D., Bondarava,M., Kinne,R.K., Kipp,H. Time-Lapse Fluorescence Microscopy of GFP-SGLT1 Reveals a High Mobility of Intracellular GLT1. *Eur. J. Cell. Biol*. 2004; 83: Suppl. 54.

Li,T., ter Veld,F., Bondarava,M., Nürnberger,H.R., Wehner,F. A novel type of hypertonicity-induced cation channel in primary human hepatocytes. *Pflüg. Arch. Eur. J. Physiol*. 2005; 449: Suppl. 1.

Wehner,F., ter Veld,F., Li,T., Endl,E., Nürnberger,H.R., Bondarava,M. Hypertonicity-induced cation channels and their putative role in proliferation and apoptosis. *5th International Symposium on Cell Volume Regulation in Health and Disease*, Copenhagen, Denmark, 2006.

Li,T., ter Veld,F., Bondarava,M., Nürnberger,H.R., Wehner,F. Characteristics and regulation of hypertonicity-induced cation channels in primary human

hepatocytes. *5th International Symposium on Cell Volume Regulation in Health and Disease*, Copenhagen, Denmark, 2006.

Bondarava,M., Li,T., Wehner,F. Molecular identification of hypertonicity-indiced cation channels in HepG2 cells. *6th International Symposium on Cell Volume Regulation in Health and Disease*, Salzburg, Austria, 2007.

Erklärung

Hiermit erkläre ich, dass ich die Arbeit selbständig verfasst und bei keiner anderen Fakultät eingereicht und dass ich keine anderen als die angegebenen Hilfsmittel verwendet habe. Es handelt sich bei der heute von mir eingereichten Dissertation um fünf in Wort und Bild völlig übereinstimmende Exemplare.

Weiterhin erkläre ich, dass digitale Abbildungen nur die originalen Daten enthalten und in keinem Fall inhaltsverändernde Bildbearbeitung vorgenommen wurde.

Bochum, den 22. November 2007

Maryna Bondarava